Recent Progress on Quaternary Copper-based Diamondoid Thermoelectric Materials

Journal:	*Materials Lab*
Manuscript ID	MATLAB-2024-0005.R1
Manuscript Type:	Review Article
Date Submitted by the Author:	03-Nov-2024
Complete List of Authors:	Zhao, Zihao; Beihang University Xie, Hongyao; Beihang University Zhao, Li-Dong; Beihang University
Keywords:	quaternary Cu-based diamondoid materials, thermoelectric performance, carrier concentration, band engineering, microstructure
Speciality:	Thermoelectrics

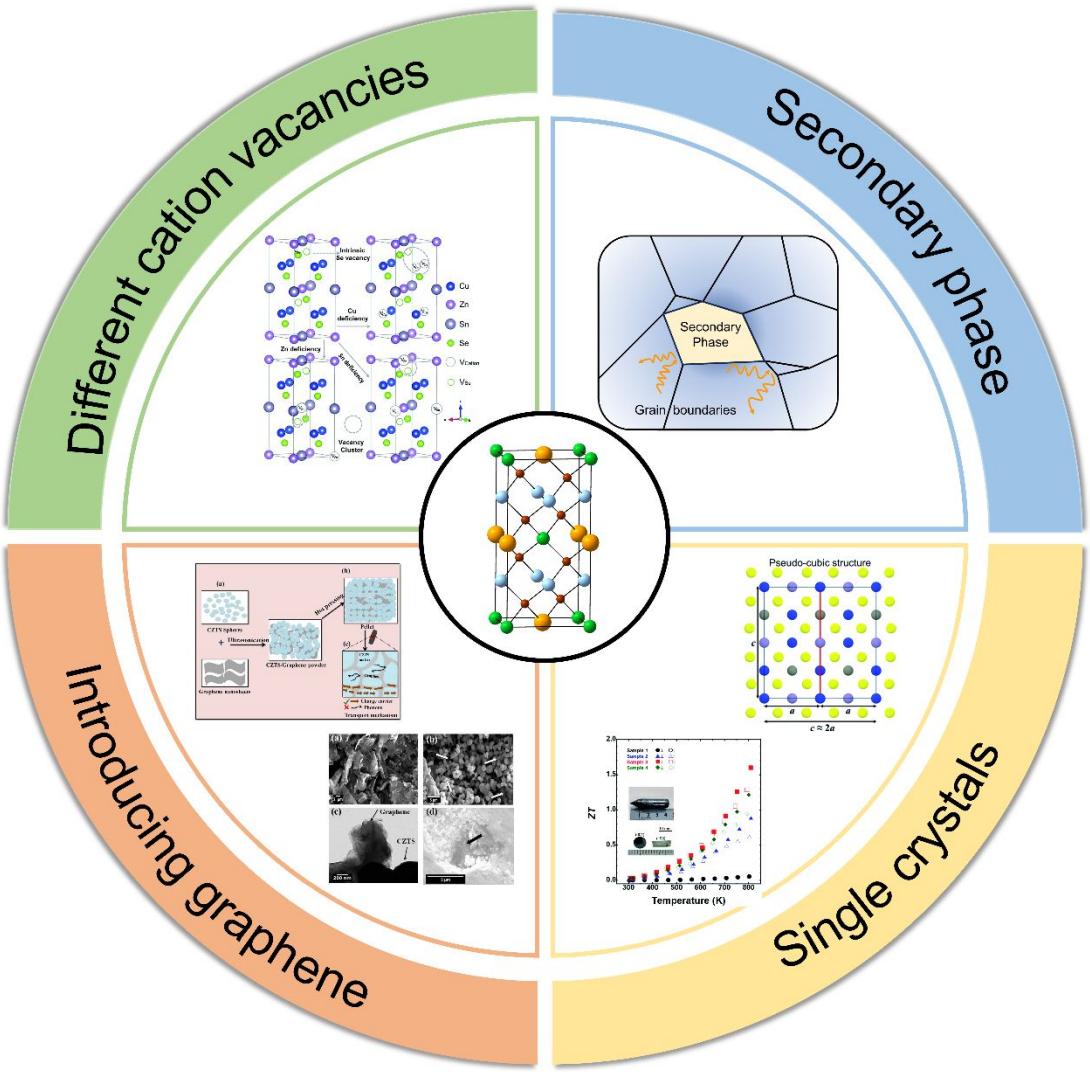

Toc

PAPER NAME

Recent Progress on Quaternary Copper-based Diamondoid Thermoelectric Materials

WORD COUNT

3575 Words

CHARACTER COUNT

21238 Characters

PAGE COUNT

15 Pages

FILE SIZE

151.2KB

SUBMISSION DATE

Oct 9, 2024 1:46 PM GMT+8

REPORT DATE

Oct 9, 2024 1:46 PM GMT+8

11% Overall Similarity

The combined total of all matches, including overlapping sources, for each database.

- 5% Internet database
- 10% Publications database
- Crossref database
- Crossref Posted Content database

Recent Progress on Quaternary Copper-based Diamondoid Thermoelectric Materials

Abstract: The rising concern on energy and environmental crises have sparked global interest in developing sustainable new energy and high-efficient energy conversion technologies. Thermoelectric technology has gained attention due to its potential for application in waste heat recovery and solid-state refrigeration. However, the application of traditional thermoelectric materials remains limited due to their expensive and toxic elemental composition. Recently, quaternary copper-based diamondoid materials have garnered significant interest due to their unique transport properties, high element abundance, and low toxicity. Many of these materials have demonstrated promising *ZT* value, positioning them as potential candidates for efficient thermoelectric applications. This paper summarizes the recent progress in copper-based quaternary diamondoid materials. We present a collection of research focused on optimizing electrical transport properties through carrier concentration tuning and band engineering, along with an overview of reducing thermal conductivity *via* microstructure enhanced phonon scattering. Finally, we analyze the current research bottlenecks in copper-based quaternary diamondoid thermoelectric materials and propose future research directions.

Keywords: quaternary Cu-based diamondoid materials, thermoelectric performance, carrier concentration, band engineering, microstructure

1 Introduction

The continuous rise in global energy demand and the depletion of unrenewable fossil fuels have made the development of sustainable new energy and high-efficiency

energy conversion technologies become the worldwide topics. Research indicates that approximately 65% of energy produced in human activities is wasted and lost as heat[1]. Thus, developing effective methods to recovery this waste heat is considered as a way to solve the energy problems. Thermoelectric materials[2-4], based on the Seebeck effect, can directly convert heat into electricity, and can also be used for solid state cooling. This makes them a promising tool for mitigating energy crises[5]. However, the low energy conversion efficiency of thermoelectric materials limits their large-scale commercial applications[6].

Generally, the performance of thermoelectric materials is mainly evaluated by the dimensionless thermoelectric figure of merit ZT, $ZT = S^2\sigma T / \kappa_{tol} = S^2\sigma T / (\kappa_e + \kappa_l)$, where S is Seebeck coefficient, σ is electrical conductivity, T is absolute temperature, κ_e is electronic thermal conductivity, κ_l is lattice thermal conductivity, and the sum of κ_e and κ_l is the total thermal conductivity of the material κ_{tol}[7-9]. $PF = S^2\sigma$, which is a power factor used to characterize the electrical transport performance of thermoelectric materials. Therefore, to improve the performance of thermoelectric materials, two main approaches are typically pursued: (1) optimizing the electrical properties; (2) reducing thermal conductivity[10, 11]. However, because of the strong inherent coupling between electrical conductivity σ, Seebeck coefficient S, and thermal conductivity κ_{tol}, it is challenging to solely regulate these parameters to achieve high thermoelectric performance[12]. For instance, increasing the carrier concentration can enhance σ, but this often reduces the S and increases κ_e, limiting the overall improvement in ZT. To overcome this, researchers employ various strategies to

decouple these properties, aiming for enhanced thermoelectric efficiency.

Since the discovery of thermoelectric effect, researchers have identified numerous high-performance thermoelectric materials. For example, SnQ (Q= S, Se)[13-16], Bi_2Te_3 alloy[8, 11, 17, 18], PbQ (Q=S, Se, Te)[19-22], Zintl phase[23], Ag_2Q (Q=S, Se, Te)[24, 25], Mg_3X_2 (X=Sb, Bi)[26, 27] , half Heusler[28], and most recently, the diamondoid compound[29-32]. Early research on diamondoid compounds primarily concentrated on their optoelectronic properties, and their thermoelectric properties did not receive sufficient attention. Until the excellent thermoelectric properties of $Cu_2ZnSnSe_4$ and $Cu_2CdSnSe_4$ were first reported by Shi[33] and Liu et al[34]. in 2009, diamondoid thermoelectric materials have attracted widespread attention from the research community. Since then, a growing number of wide bandgap diamond-like materials have been reported, such as $CuInTe_2$, $CuGaTe_2$, $CuFeS_2$, Cu_2SnSe_3, Cu_3SbSe_4, etc[30, 35-41]. These materials derive from the sphalerite structure and has the typical tetrahedral coordination geometry of diamond. This stable twisted tetrahedral structure is formed by the "cross substitution" of element, following the "eight electron rule". Since the differences in electronegativity and radius between various anions and cations, phonon scattering in this twisted lattice is greatly enhanced, resulting in low κ_l. This characteristic is important for its decent thermoelectric performance. Quaternary Cu-based diamondoid materials generally have a chemical formula of A_2BCQ_4, with a tetragonal lattice structure that exhibits a double-periodic cubic sphalerite structure along the z-direction, as shown in **Figure 1**. This complex crystal structure and elemental composition result in inherently low κ_l. In addition, the diverse elemental

composition provides it a broad scope to tune the band structure and electrical properties through chemical composition regulation. However, compared to the ternary diamondoid materials, the *ZT* value of A_2BCQ_4 compounds is lower, typically not exceeding 1.0, mainly due to their lower intrinsic σ. Therefore, a large amount of research aims to improve the electrical properties of quaternary diamondoid materials. Among these materials, Cu-based quaternary diamondoid materials have garnered the most attention. In the next, we start with introducing the recent progress in improving the electronic properties of these materials.

2 Optimization of Electrical Transport Performance

Improving the electrical properties is vital for promoting the thermoelectric performance of quaternary diamondoid materials. However, there is a strong coupling between their σ and *S*, these parameters are closely related to the carrier concentration and effective mass of the material. The σ is directly proportional to the carrier concentration and mobility:

$$\sigma = en\mu \tag{1}$$

$$n = 4\pi\left(\frac{2m^* k_B T}{h^2}\right)^{\frac{3}{2}} F_{\frac{1}{2}}(\eta) \tag{2}$$

$$\mu = \frac{2e}{3m^*}\tau_0(\lambda+1)(k_B T)^{\lambda-\frac{1}{2}}\frac{F_\lambda(\eta)}{F_{1/2}(\eta)} \tag{3}$$

Among formulas, n is carrier concentration, μ is carrier mobility, m^* is effective mass of charge carrier, k_B is Boltzmann constant, h is planck constant, η is simplified Fermi level, τ_0 is relaxation time, λ is scattering factor. Based on the single parabolic band model and the relaxation time approximation, *S* can be derived from the following

equation:

$$S = \frac{8\pi^2 k_B^2 T}{3qh^2} m^* \left(\frac{\pi}{3n}\right)^{\frac{2}{3}} \quad (4)$$

From equations 1 to 4, we can see that optimizing carrier concentration by doping and adjusting the Fermi level can significantly enhance σ. Additionally, modifying the density of states by adjusting the band structure and effective mass plays a crucial role in improving the S.

2.1 Optimization of Carrier Concentration

Optimizing the carrier concentration is one of the most direct methods to enhance electrical performance. The carrier concentration in a material is influenced by its defect states. Therefore, element doping is a common way to adjust the carrier concentration. Unlike traditional narrow bandgap thermoelectrics ($E_g \leqslant 0.5$ eV), most of Cu-based diamondoid thermoelectric materials exhibit relatively wide bandgaps, $E_g > 1$eV, as shown in **Table1**. Because of the wide bandgap, most diamondoid materials have intrinsic low carrier concentrations, and element doping is a common and useful method to increase their carrier density and σ.

Recently, many researchers have attempted various doping methods in quaternary diamondoid materials. According to the doping elements, they can be divided into intrinsic and extrinsic doping. Intrinsic doping or self-doping, occurs without introducing any other extrinsic elements, and achieve doping effect by regulating the stoichiometric ratio of the material. In Cu-based diamondoid materials, the predominant charge carriers responsible for electrical transport are holes. Given that the formation

energy of copper vacancies is relatively small, these vacancies serve as intrinsic defects and significantly influencing the electrical properties of the material. In the early report by Liu et al in 2009 on $Cu_2CdSnSe_4$[34], substituting Cd with Cu can effectively improve the σ. They found the [Cu_2Se_4] tetrahedral slabs function as electrically conducting units, while the [$SnCdSe_4$] units act as the electrically insulating structures. Thus, introducing excess Cu can not only introduce more intrinsic copper vacancies, generating more holes, but the insulating paths are also transformed into conductive ones due to the replacement of Cd with Cu. As a result, the σ of $Cu_{2.1}Cd_{0.9}SnSe_4$ achieved an impressive value of 20300 $S \cdot m^{-1}$ at room temperature, which is about six times higher than that of the pristine sample. The same strategy was successfully applied in another work in 2009[42], where excess Cu was introduced into $Cu_2ZnSnSe_4$. This result in an impressive σ of 86000 $S \cdot m^{-1}$ and achieved a groundbreaking ZT of 0.91 at 860K. Following these findings, many researchers adopted this strategy to improve the thermoelectric performance of diamondoid materials. For example, Qinghui Jiang et al[43] prepared Cu_2ZnSnS_4 samples using ball milling and hot press methods, and introduced additional Cu into the Zn sites to generate more hole carriers and improve σ. Finally, a high ZT value of 1.1 has been achieved for $Cu_{2.125}Zn_{0.875}SnS_4$. Besides, Yongkwan Dong et al[44] explored introducing larger doses of Cu to further improve the σ of the material. Although introducing more low-valence cations at high valence sites has been proven to be an effective means of improving σ, excessive doping can easily lead to the formation of secondary phases. To address this, Zhou Li et al[45] explored optimizing the carrier concentration by constructing different cation

vacancies in $Cu_2ZnSnSe_4$, as shown in **Figure 2**. They studied the effects of three types of cationic vacancies, Cu, Zn, and Sn, on electrical properties, and found that all samples exhibited a significant increase in hole concentration compared to the pristine samples. Notably, the Sn-deficient sample achieved the highest carrier concentration of 7.5×10^{19} cm^{-3}, resulting in an σ of 4700 $S\cdot m^{-1}$.

In addition to intrinsic doping, introducing extrinsic elements to increase the carrier concentration is a commonly used and effective optimization method. For example, X. Y. Shi et al[33] attempted to dope In at Sn site in $Cu_2ZnSnSe_4$, achieving a high carrier concentration that significantly improved the σ of the material, resulting in a record high *ZT* of 0.95 at 850K. Similarly, F. S. Liu et al[46] explored the role of doping Mn at Cd site in $Cu_2CdSnSe_4$ through experiment and theoretical calculation. They found that Mn doping causes the Fermi level to shift towards the valence band, resulting in a higher hole concentration while the carrier mobility decreases with increasing Mn content, ultimately leading to an increase in σ. Bo Wang et al[47] also achieved a similar effect by doping Ga at the Sn site in $Cu_2CdSnSe_4$. This strategy was also used in $Cu_2CdSn_{0.9}In_{0.1}Se_4$[48], $Cu_2MnSn_{0.95}In_{0.05}Se_4$[49] and $Cu_2ZnSn_{0.95}Ga_{0.05}Se_4$[50], further demonstrating the effectiveness of extrinsic doping in enhancing the thermoelectric performance of quaternary diamondoid materials.

2.2 Optimization of Carrier Mobility

It is well known that, the carrier mobility of a material is closely related to the effective mass and scattering mechanisms. Therefore, a large amount of research on

carrier mobility optimization has focused on these aspects. For example, Q. Song et al[51] optimized the lower intrinsic mobility of materials by manipulating the intrinsic lattice defects in $Cu_2FeSnSe_4$. They calculated the defect formation energies under both Cu-poor and Cu-rich conditions and identified the dominated defect types in $Cu_2FeSnSe_4$. In the case of Cu deficiency (**Figure 3a**), the defect formation energy of Cu vacancies is negative, indicating that Cu vacancies spontaneously occur during material preparation. Since the Cu vacancy is electronegative, making them to disrupt the original periodicity of the lattice and introduce additional ionized impurity scattering centers, thus reducing the carrier mobility, as shown in **Figure 3c**.

In contrast, they found that under Cu-rich condition, the defect formation energy of Cu atoms occupying Fe sites (Cu_{Fe} anti-site defect) is lower than that of Cu vacancies, indicating the Cu_{Fe} anti-site defect is dominant, as shown in **Figure 3b**. This defect is electrically neutral, so it causes only minimal disruption to the charge transport (**Figure 3d**). As a result, carrier mobility is less affected by scattering. Through carefully controlling the Cu content, they successfully achieved a synergistic optimization of both carrier mobility and carrier concentration. Furthermore, doping In into $Cu_2MnSnSe_4$ can also improve the carrier mobility of the material[49]. This enhancement may be attributed to the optimization of band structure. In addition, by studying the transport properties of $Cu_2CoSnSe_4$ and Cu_2CoSnS_4. Taras Parashchuk et al[52] found that the selenide compound exhibited higher symmetry than its sulfide analogue, featuring with the bond angles closer to the ideal tetrahedral angle of 109.5°, this contribute to a higher carrier mobility.

Improving the electrical transport properties by introducing a secondary phase is a novel method. For example, Sarita Devi Sharma et al[53] improved the thermoelectric properties of Cu_2ZnSnS_4 by adding graphene nanosheets (GNs) into the matrix, as shown in **Figure 4**. The increase in σ is attributed to the formation of percolation channels created by the 2D graphene, which facilitates the transport of charge carriers. In this case, even small amount of GNs can produce a significant percolation effect. Additionally, the graphene nanosheets can exhibit a doping effect and moderately increases the carrier density of the material.

Similarly, Arslan Ashfaq et al[54] prepared a series of Al-doped Cu_2ZnSnS_4 nanoparticles using the hydrothermal method, and found the extra Al effectively increases the σ of the material. This is because a small amount of Al particles diffuses into the gap of the matrix, forming bridge that allow charge carriers to pass freely through the grain boundaries, thus, increase the carrier concentration and mobility simultaneously.

2.3 Optimization of Seebeck Coefficient

The S is closely related to the density of states effective mass and carrier concentration. Although reducing carrier concentration is able to increase the S, it simultaneously lowers the σ. Therefore, band structure optimization emerges as a practical option to boost the S without compromising the σ. Cu-based quaternary diamondoid materials can exhibit two distinct crystal structures, the highly ordered Stannite and the disordered Kesterite. The symmetry of these crystal structures directly impacts the band structure of materials. Various methods have been developed to

optimize the band structure and transport properties through manipulating the crystal structure. Eleonora Isotta et al[55] demonstrated that the transition from an ordered to a disordered structure in Cu_2ZnSnS_4 improves the thermoelectric properties of materials, primarily due to alterations in the electronic band structure as shown in **Figure 5**. They found a second-order reversible phase transition occurring near 533K. **Figure 5a** shows that the *S* increases sharply around the transition temperature, attributed to the higher symmetry associated with the disordered structure. At the same time, the σ of the material dramatically drops at the phase transition temperature, as shown in **Figure 5b**. Through the electronic band calculation, they found that in disordered structures, the energy difference among the first three valence bands decrease, the top of the valence band flattens, and the band gap also decreases, as shown in the **Figure 5c**. Following this, Akira Nagaoka et al[56] employed a pseudo-cubic strategy to enhance the thermoelectric performance of Cu_2ZnSnS_4 single crystal, as shown in **Figure 6**. They obtained the degenerate electron energy bands in the pseudo-cubic structure, resulting in a high *S* and a remarkable *ZT* value of 1.6 at 800K in the material.

In addition, several methods can effectively improve the *S* of materials without altering their band structure. For example, by introducing energy barriers at the interface through doping or incorporation of secondary phase, low-energy carriers would be greatly scattered while high-energy carriers can pass through, achieving the goal of improving *S*. Qiufan Chen et al[57] doped Ag atoms into $Cu_2CdSnSe_4$ using a chemical method, successfully embedding a disordered sphalerite structure within the ordered sphalerite phase. This modification caused the energy band at the interface to

bend, thereby generating energy barriers that effectively scatter low-energy carriers. As a result, both the S and σ were improved. Jolly Jacob et al[58] adopted a similar strategy by doping Cd into Cu_2ZnSnS_4 and found that the S increased with adding Cd. They found that, Cd doping led to the formation of Cu-based secondary phases. These secondary phases serve as effective filters for low-energy carriers, while allowing only high-energy carriers to pass through, thereby improving the performance of material. Additionally, introducing spin entropy by doping magnetic particles such as Ni[59] or elements such as Pb and Te[60] can effectively increase the effective mass and improve the S of the material.

3 Optimization of Thermal Transport Performance

We know that the transfer of thermal energy is mainly achieved through lattice vibrations and carrier transport, with the former represented as lattice thermal conductivity κ_l and the latter as electronic thermal conductivity κ_e. They can be represented as:

$$\kappa_l = \frac{1}{3} C_V \upsilon l \quad (5)$$

$$\kappa_e = L\sigma T \quad (6)$$

In the above equation, C_v is specific heat at constant volume of materials, υ is phonon velocity, l is mean free path of phonon collision[61], L is Lorentz constant. Although the complex crystal structure and elemental composition of Cu-based quaternary diamondoid materials result in relatively low intrinsic thermal conductivity, there is still room for further optimization. Unlike κ_e, κ_l is almost independent of other electronic

transport parameters, and can be regulated independently. To this end, many researchers have focused on reducing the κ_l to improve the thermoelectric performance. Defect control and microstructure design are two effective methods for reducing κ_l.

3.1 Defect Control

Compared to C_v and υ, the l is easier to regulate, particularly through controlling the defects state in the material. So far, introducing appropriate defects into the lattice to reduce the l has remained the main strategy for suppressing κ_l. The impact of point defects mainly lies in the fluctuation of the mass field caused by different atomic masses and the fluctuation of the stress field caused by different atomic radii. The larger the difference, the stronger the scattering effect on high-frequency phonons, and the better the result in reducing κ_l. For example, Qiufan Chen et al[57] prepared Ag-doped $Cu_2CdSnSe_4$ using a chemical method, which introduced Ag_{Cu} point defects into the matrix, distorting the crystal structure and enhancing the phonon scattering. In addition, Qingfeng Song et al[62] introduced excess Cu into $Cu_2MnSnSe_4$, increasing local lattice distortion and suppressing κ_l. Studies also indicate that replacing Zn with Co in $Cu_2ZnSnSe_4$ increases point defects, reduces phonon relaxation time, and thus decrease κ_l [63]. Besides, anionic substitution significantly reduces the κ_l of $Cu_2ZnGeSe_{4-x}S_x$[64], primarily due to the disorder caused by substitution. Ultra-low κ_l can also be achieved in the locally disordered $Cu_{2+x}Zn_{1-x}SnS_4$[43], which is mainly attributed to the highly disordered arrangement of Cu and Zn in the lattice, causing phonon localization and shortening the phonon mean free path. Some researchers also use lattice strain to

regulate the thermoelectric properties of materials[65]. They introduce lattice strain by creating dislocations, which reduce the relaxation time of phonons and enhance their scattering, as shown in **Figure 7**.

3.2 Microstructure Design

In addition to introducing point defects, microstructure design, such as nano precipitate, nanocrystalline material, and secondary phase boundary, can also reduce κ_l. For example, Feng-Jia Fan et al[66] synthesized $Cu_2CdSnSe_4$ nanocrystals through colloidal synthesis and prepared bulk materials by hot pressing. In their work, the nanocrystals generated more grain boundaries, significantly enhancing phonon scattering. This ultimately resulted in a thermal conductivity of 1.7 W m^{-1} K^{-1}at room temperature, which is about 40% lower than that of the bulk sample prepared by solid-state reaction. After that, Kaya Wei et al[67] reported the preparation of nanostructured $Cu_2ZnSnSe_4$ and $Ag_2ZnSnSe_4$, once again confirming the impact of nanomaterials on the κ_l of these materials. Combining bulk materials with nanocrystals can reduce thermal conductivity while maintaining the high electrical properties of the bulk material. Qiufan Chen et al[68] prepared $Cu_2CdSnSe_4$ nanocrystals suing colloidal synthesis and added these nanocrystals into the $Cu_2CdSnSe_4$ matrix, as shown in **Figure 8**. They found that this hierarchical architecture is able to suppress the thermal conductivity while preserve the decent electrical properties. The increased grain boundaries and embedded nanocrystals significantly enhanced phonon scattering, especially the latter serving as an additional scattering center that effectively scatter medium to long wavelength phonons, thereby reducing κ_l. Himanshu Nautiyal et al[69]

synthesized disordered nanostructured polycrystals of Cu_2ZnSnS_4 and $Cu_2ZnSnSe_4$ through high-energy reaction mechanical alloying, achieving a low thermal conductivity of 0.2 W m^{-1} K^{-1}. Similar studies have also been conducted by Binayak Mukherjee et al[70], who obtained cubic $Cu_2ZnSnSe_4$ nanostructures with a low thermal conductivity of 0.21W m^{-1} K^{-1}.

The optimization of thermal conductivity through the introduction of secondary phase grain boundary engineering has also been proven to be an effective method. The interface between the secondary phase and the matrix generates strong phonon scattering. Yingcai Zhu et al[71] replaced Sn with Pb in $Cu_2ZnSnSe_4$ and found that Pb primarily exists in the PbSe framework, distributed as a secondary phase at grain boundaries, as shown in **Figure 9**. The phase interface between the secondary phase and the matrix has a strong scattering effect on phonons. Additionally, the smaller grain size of the secondary phase increases the density of grain boundaries and further reduces the κ_l. Furthermore, the composite of CdSe and $Cu_2CdSnSe_4$ forms a coherent phase interface, allowing charge carriers to pass through while scattering phonons across a wide frequency spectrum[72]. The Cd vaporization during the hot pressing, creating nanopores in the material that introduce additional scattering centers, significantly reducing the κ_l.

4 Summary and Outlook

Recently, diamondoid thermoelectric materials have gained significant attention due to their unique electronic and thermal transport properties. Although their

thermoelectric performance has yet to reach the levels of traditional thermoelectric materials, they are still a new star with great research potential. This article focuses on Cu-based quaternary diamondoid materials and provides a collection of recent progress and a comprehensive view of the optimization strategies for improving their electrical and thermal properties. We have thoroughly discussed the influence of various defects on the carrier concentration, carrier mobility and the band structure of the Cu-based quaternary diamondoid materials. Additionally, we have summarized a series of effective methods to enhance the phonon scattering and suppress the thermal conductivity. Overall, improving the carrier mobility while further reducing the thermal conductivity is critical for achieving high thermoelectric performance in these materials. In this context, the recently proposed off-centering effect may offer a new perspective and provide promising pathways for future optimization. In summary, although significant progress has been made in promoting the thermoelectric performance of these systems, many challenges remain unresolved. We hope this review provide fresh insights and sparks new ideas for further improving the thermoelectric performance of these promising materials.

11% Overall Similarity

Top sources found in the following databases:

- 5% Internet database
- 10% Publications database
- Crossref database
- Crossref Posted Content database

TOP SOURCES

The sources with the highest number of matches within the submission. Overlapping sources will not be displayed.

1	Ctirad Uher. "Materials Aspect of Thermoelectricity", CRC Press, 2019 Publication	1%
2	Q. Song, P. Qiu, H. Chen, K. Zhao, M. Guan, Y. Zhou, T.-R. Wei, D. Ren, L... Crossref	<1%
3	Z. Z. Zhou, Huijun Liu, Dengdong Fan, B. Y. Zhao, C. Y. Sheng, G. H. Ca... Crossref	<1%
4	Lijie Chang, Qi Chen, Yao Wang, Dayi Zhou, Xin Fan, Xinjian Li, Yuewen ... Crossref	<1%
5	ri.conicet.gov.ar Internet	<1%
6	Jolly Jacob, Hafiz T. Ali, A. Ali, Khurram Mehboob, Arslan Ashfaq, Salm... Crossref	<1%
7	qmro.qmul.ac.uk Internet	<1%
8	Bin Chen, Xiang He Peng, Jing Hong Fan. "Research of the Herringbone... Crossref	<1%
9	Chun Feng, Ruizhe Li, Yonggang Liu, Le Liu, Wenwen Song, Fangfang Z... Crossref	<1%

10	Gopalakrishnan Sai Gautam, Thomas P. Senftle, Emily A. Carter. "Unde... Crossref	<1%
11	Kim, I.H.. "Electronic transport properties of Fe-doped CoSb"3 prepared... Crossref	<1%
12	V. V. Astanin. "Localization of plastic deformation in high-speed shock ... Crossref	<1%
13	Chengwei Gao, Jiahui Zhang, Chengmiao He, Yanqing Fu et al. " Unveili... Crossref	<1%
14	journals.iucr.org Internet	<1%
15	paper.edu.cn Internet	<1%
16	science.gov Internet	<1%
17	Meiling Ma, Yingrui Sui, Fancong Zeng, Na Zhao, Tianyue Wang, Zhanw... Crossref	<1%
18	pubs.rsc.org Internet	<1%
19	Qiang Zhang, Yun Zheng, Xianli Su, Kang Yin, Xinfeng Tang, Ctirad Uher... Crossref	<1%
20	V.P.N. Prasadi, G.M. Somaratne, B.D. Rohitha Prasantha, C.K. Abeyrath... Crossref	<1%
21	Yiqun Zhang, Yi Shi, Lin Pu, Junzhuan Wang, Lijia Pan, Youdou Zheng. "... Crossref	<1%

22	link.springer.com Internet	<1%
23	researchgate.net Internet	<1%
24	Cong Yin, Hangtian Liu, Qing Hu, Jing Tang, Yanzhong Pei, Ran Ang. "T... Crossref	<1%
25	Sabah K. Bux, Jean-Pierre Fleurial, Richard B. Kaner. "Nanostructured ... Crossref	<1%
26	Shengbo Yin, Cuihua Zhao, Bo-Ping Zhang, Wenbo Zhao, Chencheng Z... Crossref	<1%
27	nature.com Internet	<1%
28	David Michael Rowe. "Modules, Systems, and Applications in Thermoel... Publication	<1%

Dear Editor,

Please find our revised paper **MATLAB-2024-0005** titled "**Recent Progress on Quaternary Copper-based Diamondoid Thermoelectric Materials**". We appreciate the careful examination of our paper by the referees and are grateful for their comments and constructive criticism.

We have revised our paper (**modifications are highlighted in yellow**) and provided a point-by-point response and description of the revisions.

Description of the revisions:

1. The accurate use of symbols has been corrected and added to page 2, page 22 and pages 27 - 29 in the revised manuscript. (Reviewer #1, Comment #1)
2. The relevant grammar expressions in the manuscript have been modified and added to pages 3 - 9 and pages 13 -14 in the revised manuscript. (Reviewer #1, Comment #2, Comment #3, Comment #4, Comment #5; Reviewer #2, Comment #4)
3. The discussion section regarding Figs. 3e and 3f has been added to page 8 in the revised manuscript. (Reviewer #2, Comment #2)

We trust that with the changes made to text and figure, the paper is now suitable for publication in ***Materials Lab***.

Thank you again and we are looking forward to hearing from you.

Best regards.
Hongyao Xie

Reviewer(s)' Comments to Author:

Reviewer: 1

This paper summarized the recent progress on diamondoid $Cu_2ZnSnSe_4$ thermoelectric materials, introduced a series of optimization strategies and outlined the current challenges faced by the material. I think this work provide some new ideas for further improving the performance of $Cu_2ZnSnSe_4$ system. I recommend this work to be published after some minor revisions. My detailed comment and suggestions are listed below.

Question/Comments 1: The authors mentioned that 'total thermal conductivity of the material κtol'. Please correct it to 'total thermal conductivity of the material κtot'. See page 2 and elsewhere in the text.

Reply: Thank you for the reminder. The symbol of total thermal conductivity was revised.

Question/Comments 2: The authors mentioned that 'in 2009, diamondoid thermoelectric materials have attracted widespread attention from the research community'. Please correct it to 'In 2009, diamondoid thermoelectric materials have attracted widespread attention from the research community'. See page 3.

Reply: Thank you for the reminder. The corresponding statement was corrected.

Question/Comments 3: The authors mentioned 'carrier density', please change it to 'carrier concentrations' See page 5.

Reply: Thanks for the suggestion, we carefully revised this issue and paid attention to the consistency of the wording in the manuscript.

Question/Comments 4: The authors mentioned 'Given that the formation energy of copper vacancies is relatively small, these vacancies serve as intrinsic defects and significantly influencing the electrical properties of the material', please change it to 'Given that the formation energy of copper vacancies is relatively small, these vacancies serve as intrinsic defects significantly influencing the electrical properties of the material'. See page 6.

Reply: Thanks for the suggestion. The corresponding statement was corrected.

Question/Comments 5: The authors mentioned 'Additionally, the graphene nanosheets can exhibit a doping effect and moderately increases the carrier density of the material'. Please change 'increases' to 'increase'. See page 9.

Reply: Thanks for the suggestion, This issue was revised.

Reviewer: 2

In this paper, the authors discuss quaternary copper-based diamondoid materials for thermoelectric applications. The paper reviews progress in improving their electrical transport properties and reducing thermal conductivity while identifying current research challenges and suggesting future directions. This review is important because copper-based diamondoid materials offer advantages such as elemental abundance, low toxicity, and unique transport characteristics. The paper is well-written and includes all the key milestones in the development of copper-based diamondoid materials, making it a valuable reference for future studies. I recommend accepting this paper for publication after addressing the following issues.

Question/Comments 1: On Page 8, the authors mention that CuFe is an electrically neutral anti-site defect. However, in Fig. 3e, the carrier concentration nearly doubles in Cu2+xFe1-xSnSe4 when x changes from 0 to 0.1. What could be the potential reason for this systematic change in carrier concentration?

Reply: Thanks for the suggestion. The statement of "CuFe is electrically neutral anti-site defect" is referenced from the corresponding literature. and we recognize that this characterization may be misleading. In reality, when Cu is doped into Fe site, most of the Cu behave as +2, with a small fraction exhibiting +1 oxidation state. Consequently, the hole concentration slightly increases with adding Cu. But the increment is very minimal, indicating that the CuFe anti-site defect is nearly electrically neutral. We have corrected the corresponding statement to reflect this understanding.

Question/Comments 2: In the manuscript, Figs. 3e and 3f are present but not discussed in the text. I recommend that the authors either remove these figures or add a relevant discussion if they are important.

Reply: Thanks for the suggestion. We added a relevant discussion on page 8 for Figs. 3e and 3f in order to demonstrate the effectiveness of this regulatory strategy in improving the electrical properties of materials.

Question/Comments 3: On page 9, the authors state that adding graphene nanosheets to Cu2ZnSnS4 significantly improves electrical conductivity. Does this result in anisotropic transport properties in the composite, as graphene sheets can become highly oriented after hot pressing?

Reply: Thanks for the suggestion. Some layer materials, such as BiCuSeO, introducing the graphene can enhance their orientation and results in anisotropic transport properties. In contrast, diamondoid compounds have a pseudo-cubic structure and exhibit weak anisotropy. Adding graphene to Cu2ZnSnS4 does not improve the preferred orientation of the matrix. Moreover, the SEM images reveal that the distribution of graphenes within Cu2ZnSnS4 is uniform and their orientation is random. Therefore, while the hot pressing of graphene into Cu2ZnSnS4 may induce some degree of anisotropic, it is unlikely to be significant.

Question/Comments 4: There are a few minor grammatical issues that need to be addressed. On page 14, it should be 'using' instead of 'suing,' 'preserving' instead of

'preserve,' 'additional scattering centers' instead of 'an additional scattering center,' and 'the introduction of secondary phase grain boundary engineering' is an awkward expression. Is this correct? Should it be 'grain boundary engineering through the introduction of a secondary phase'?

Reply: Thanks for the suggestion. We greatly appreciate you pointing out these grammar issues. We have double checked the manuscript and corrected all mistakes.

Recent Progress on Quaternary Copper-based Diamondoid Thermoelectric Materials

Zihao Zhao[1], Hongyao Xie[1,*], Li-Dong Zhao[1,*]

[1]*School of Materials Science and Engineering, Beihang University, Beijing 100191, China.*

E-mail: xiehongyao@buaa.edu.cn; *zhaolidong@buaa.edu.cn*

Abstract: The rising concern on energy and environmental crises have sparked global interest in developing sustainable new energy and high-efficient energy conversion technologies. Thermoelectric technology has gained attention due to its potential for application in waste heat recovery and solid-state refrigeration. However, the application of traditional thermoelectric materials remains limited due to their expensive and toxic elemental composition. Recently, quaternary copper-based diamondoid materials have garnered significant interest due to their unique transport properties, high element abundance, and low toxicity. Many of these materials have demonstrated promising *ZT* value, positioning them as potential candidates for efficient thermoelectric applications. This paper summarizes the recent progress in copper-based quaternary diamondoid materials. We present a collection of research focused on optimizing electrical transport properties through carrier concentration tuning and band engineering, along with an overview of reducing thermal conductivity *via* microstructure enhanced phonon scattering. Finally, we analyze the current research bottlenecks in copper-based quaternary diamondoid thermoelectric materials and propose future research directions.

Keywords: quaternary Cu-based diamondoid materials, thermoelectric performance, carrier concentration, band engineering, microstructure

1 Introduction

The continuous rise in global energy demand and the depletion of unrenewable fossil fuels have made the development of sustainable new energy and high-efficiency energy conversion technologies become the worldwide topics. Research indicates that approximately 65% of energy produced in human activities is wasted and lost as heat[1]. Thus, developing effective methods to recovery this waste heat is considered as a way to solve the energy problems. Thermoelectric materials[2-4], based on the Seebeck effect, can directly convert heat into electricity, and can also be used for solid state cooling. This makes them a promising tool for mitigating energy crises[5]. However, the low energy conversion efficiency of thermoelectric materials limits their large-scale commercial applications[6].

Generally, the performance of thermoelectric materials is mainly evaluated by the dimensionless thermoelectric figure of merit ZT, $ZT = S^2\sigma T / \kappa_{tot} = S^2\sigma T / (\kappa_e + \kappa_l)$, where S is Seebeck coefficient, σ is electrical conductivity, T is absolute temperature, κ_e is electronic thermal conductivity, κ_l is lattice thermal conductivity, and the sum of κ_e and κ_l is the total thermal conductivity of the material κ_{tot}[7-9]. $PF = S^2\sigma$, which is a power factor used to characterize the electrical transport performance of thermoelectric materials. Therefore, to improve the performance of thermoelectric materials, two main approaches are typically pursued: (1) optimizing the electrical properties; (2) reducing thermal conductivity[10, 11]. However, because of the strong inherent coupling between electrical conductivity σ, Seebeck coefficient S, and thermal conductivity κ_{tot}, it is challenging to solely regulate these parameters to achieve high

thermoelectric performance[12]. For instance, increasing the carrier concentration can enhance σ, but this often reduces the S and increases κ_e, limiting the overall improvement in ZT. To overcome this, researchers employ various strategies to decouple these properties, aiming for enhanced thermoelectric efficiency.

Since the discovery of thermoelectric effect, researchers have identified numerous high-performance thermoelectric materials. For example, SnQ (Q= S, Se)[13-16], Bi_2Te_3 alloy[8, 11, 17, 18], PbQ (Q=S, Se, Te)[19-22], Zintl phase[23], Ag_2Q (Q=S, Se, Te)[24, 25], Mg_3X_2 (X=Sb, Bi)[26, 27] , half Heusler[28], and most recently, the diamondoid compound[29-32]. Early research on diamondoid compounds primarily concentrated on their optoelectronic properties, and their thermoelectric properties did not receive sufficient attention. Until the excellent thermoelectric properties of $Cu_2ZnSnSe_4$ and $Cu_2CdSnSe_4$ were first reported by Shi[33] and Liu et al[34]. In 2009, diamondoid thermoelectric materials have attracted widespread attention from the research community. Since then, a growing number of wide bandgap diamond-like materials have been reported, such as $CuInTe_2$, $CuGaTe_2$, $CuFeS_2$, Cu_2SnSe_3, Cu_3SbSe_4, etc[30, 35-41]. These materials derive from the sphalerite structure and has the typical tetrahedral coordination geometry of diamond. This stable twisted tetrahedral structure is formed by the "cross substitution" of element, following the "eight electron rule". Since the differences in electronegativity and radius between various anions and cations, phonon scattering in this twisted lattice is greatly enhanced, resulting in low κ_l. This characteristic is important for its decent thermoelectric performance. Quaternary Cu-based diamondoid materials generally have a chemical formula of A_2BCQ_4, with a

tetragonal lattice structure that exhibits a double-periodic cubic sphalerite structure along the z-direction, as shown in **Figure 1**. This complex crystal structure and elemental composition result in inherently low κ_l. In addition, the diverse elemental composition provides it a broad scope to tune the band structure and electrical properties through chemical composition regulation. However, compared to the ternary diamondoid materials, the *ZT* value of A_2BCQ_4 compounds is lower, typically not exceeding 1.0, mainly due to their lower intrinsic σ. Therefore, a large amount of research aims to improve the electrical properties of quaternary diamondoid materials. Among these materials, Cu-based quaternary diamondoid materials have garnered the most attention. In the next, we start with introducing the recent progress in improving the electronic properties of these materials.

2 Optimization of Electrical Transport Performance

Improving the electrical properties is vital for promoting the thermoelectric performance of quaternary diamondoid materials. However, there is a strong coupling between their σ and *S*, these parameters are closely related to the carrier concentration and effective mass of the material. The σ is directly proportional to the carrier concentration and mobility:

$$\sigma = en\mu \tag{1}$$

$$n = 4\pi\left(\frac{2m^* k_B T}{h^2}\right)^{\frac{3}{2}} F_{\frac{1}{2}}(\eta) \tag{2}$$

$$\mu = \frac{2e}{3m^*}\tau_0(\lambda+1)(k_B T)^{\lambda-\frac{1}{2}}\frac{F_\lambda(\eta)}{F_{1/2}(\eta)} \tag{3}$$

Among formulas, n is carrier concentration, μ is carrier mobility, $m^*$is effective mass of charge carrier, k_B is Boltzmann constant, h is planck constant, η is simplified Fermi level, τ_0 is relaxation time, λ is scattering factor. Based on the single parabolic band model and the relaxation time approximation, S can be derived from the following equation:

$$S = \frac{8\pi^2 k_B^2 T}{3eh^2} m^* \left(\frac{\pi}{3n}\right)^{\frac{2}{3}} \quad (4)$$

From equations 1 to 4, we can see that optimizing carrier concentration by doping and adjusting the Fermi level can significantly enhance σ. Additionally, modifying the density of states by adjusting the band structure and effective mass plays a crucial role in improving the S.

2.1 Optimization of Carrier Concentration

Optimizing the carrier concentration is one of the most direct methods to enhance electrical performance. The carrier concentration in a material is influenced by its defect states. Therefore, element doping is a common way to adjust the carrier concentration. Unlike traditional narrow bandgap thermoelectrics ($E_g \leq 0.5$ eV), most of Cu-based diamondoid thermoelectric materials exhibit relatively wide bandgaps, $E_g > 1$eV, as shown in **Table1**. Because of the wide bandgap, most diamondoid materials have intrinsic low carrier concentrations, and element doping is a common and useful method to increase their carrier concentrations and σ.

Recently, many researchers have attempted various doping methods in quaternary

diamondoid materials. According to the doping elements, they can be divided into intrinsic and extrinsic doping. Intrinsic doping or self-doping, occurs without introducing any other extrinsic elements, and achieve doping effect by regulating the stoichiometric ratio of the material. In Cu-based diamondoid materials, the predominant charge carriers responsible for electrical transport are holes. Given that the formation energy of copper vacancies is relatively small, these vacancies serve as intrinsic defects significantly influencing the electrical properties of the material. In the early report by Liu et al in 2009 on $Cu_2CdSnSe_4$[34], substituting Cd with Cu can effectively improve the σ. They found the [Cu_2Se_4] tetrahedral slabs function as electrically conducting units, while the [$SnCdSe_4$] units act as the electrically insulating structures. Thus, introducing excess Cu can not only introduce more intrinsic copper vacancies, generating more holes, but the insulating paths are also transformed into conductive ones due to the replacement of Cd with Cu. As a result, the σ of $Cu_{2.1}Cd_{0.9}SnSe_4$ achieved an impressive value of 20300 $S \cdot m^{-1}$ at room temperature, which is about six times higher than that of the pristine sample. The same strategy was successfully applied in another work in 2009[42], where excess Cu was introduced into $Cu_2ZnSnSe_4$. This result in an impressive σ of 86000 $S \cdot m^{-1}$ and achieved a groundbreaking ZT of 0.91 at 860K. Following these findings, many researchers adopted this strategy to improve the thermoelectric performance of diamondoid materials. For example, Qinghui Jiang et al[43] prepared Cu_2ZnSnS_4 samples using ball milling and hot press methods, and introduced additional Cu into the Zn sites to generate more hole carriers and improve σ. Finally, a high ZT value of 1.1 has been achieved for $Cu_{2.125}Zn_{0.875}SnS_4$.

Besides, Yongkwan Dong et al[44] explored introducing larger doses of Cu to further improve the σ of the material. Although introducing more low-valence cations at high valence sites has been proven to be an effective means of improving σ, excessive doping can easily lead to the formation of secondary phases. To address this, Zhou Li et al[45] explored optimizing the carrier concentration by constructing different cation vacancies in $Cu_2ZnSnSe_4$, as shown in **Figure 2**. They studied the effects of three types of cationic vacancies, Cu, Zn, and Sn, on electrical properties, and found that all samples exhibited a significant increase in hole concentration compared to the pristine samples. Notably, the Sn-deficient sample achieved the highest carrier concentration of 7.5×10^{19} cm^{-3}, resulting in an σ of 4700 $S\cdot m^{-1}$.

In addition to intrinsic doping, introducing extrinsic elements to increase the carrier concentration is a commonly used and effective optimization method. For example, X. Y. Shi et al[33] attempted to dope In at Sn site in $Cu_2ZnSnSe_4$, achieving a high carrier concentration that significantly improved the σ of the material, resulting in a record high *ZT* of 0.95 at 850K. Similarly, F. S. Liu et al[46] explored the role of doping Mn at Cd site in $Cu_2CdSnSe_4$ through experiment and theoretical calculation. They found that Mn doping causes the Fermi level to shift towards the valence band, resulting in a higher hole concentration while the carrier mobility decreases with increasing Mn content, ultimately leading to an increase in σ. Bo Wang et al[47] also achieved a similar effect by doping Ga at the Sn site in $Cu_2CdSnSe_4$. This strategy was also used in $Cu_2CdSn_{0.9}In_{0.1}Se_4$[48], $Cu_2MnSn_{0.95}In_{0.05}Se_4$[49] and $Cu_2ZnSn_{0.95}Ga_{0.05}Se_4$[50], further demonstrating the effectiveness of extrinsic doping in enhancing the thermoelectric

performance of quaternary diamondoid materials.

2.2 Optimization of Carrier Mobility

It is well known that, the carrier mobility of a material is closely related to the effective mass and scattering mechanisms. Therefore, a large amount of research on carrier mobility optimization has focused on these aspects. For example, Q. Song et al[51] optimized the lower intrinsic mobility of materials by manipulating the intrinsic lattice defects in $Cu_2FeSnSe_4$. They calculated the defect formation energies under both Cu-poor and Cu-rich conditions and identified the dominated defect types in $Cu_2FeSnSe_4$. In the case of Cu deficiency (**Figure 3a**), the defect formation energy of Cu vacancies is negative, indicating that Cu vacancies spontaneously occur during material preparation. Since the Cu vacancy is electronegative, making them to disrupt the original periodicity of the lattice and introduce additional ionized impurity scattering centers, thus reducing the carrier mobility, as shown in **Figure 3c**.

In contrast, they found that under Cu-rich condition, the defect formation energy of Cu atoms occupying Fe sites (Cu_{Fe} anti-site defect) is lower than that of Cu vacancies, indicating the Cu_{Fe} anti-site defect is dominant, as shown in **Figure 3b**. This defect is almost electrically neutral, so it causes only minimal disruption to the charge transport (**Figure 3d**). As a result, carrier mobility is less affected by scattering. Through carefully controlling the Cu content, they successfully achieved a synergistic optimization of both carrier mobility and carrier concentration, as shown in **Figure 3e**. And ultimately, it increased the conductivity of the material by about 2.5 times, as

shown in **Figure 3f**. Furthermore, doping In into $Cu_2MnSnSe_4$ can also improve the carrier mobility of the material[49]. This enhancement may be attributed to the optimization of band structure. In addition, by studying the transport properties of $Cu_2CoSnSe_4$ and Cu_2CoSnS_4. Taras Parashchuk et al[52] found that the selenide compound exhibited higher symmetry than its sulfide analogue, featuring with the bond angles closer to the ideal tetrahedral angle of 109.5°, this contribute to a higher carrier mobility.

Improving the electrical transport properties by introducing a secondary phase is a novel method. For example, Sarita Devi Sharma et al[53] improved the thermoelectric properties of Cu_2ZnSnS_4 by adding graphene nanosheets (GNs) into the matrix, as shown in **Figure 4**. The increase in σ is attributed to the formation of percolation channels created by the 2D graphene, which facilitates the transport of charge carriers. In this case, even small amount of GNs can produce a significant percolation effect. Additionally, the graphene nanosheets can exhibit a doping effect and moderately increase the carrier concentrations of the material.

Similarly, Arslan Ashfaq et al[54] prepared a series of Al-doped Cu_2ZnSnS_4 nanoparticles using the hydrothermal method, and found the extra Al effectively increases the σ of the material. This is because a small amount of Al particles diffuses into the gap of the matrix, forming bridge that allow charge carriers to pass freely through the grain boundaries, thus, increase the carrier concentration and mobility simultaneously.

2.3 Optimization of Seebeck Coefficient

The *S* is closely related to the density of states effective mass and carrier concentration. Although reducing carrier concentration is able to increase the *S*, it simultaneously lowers the σ. Therefore, band structure optimization emerges as a practical option to boost the *S* without compromising the σ. Cu-based quaternary diamondoid materials can exhibit two distinct crystal structures, the highly ordered Stannite and the disordered Kesterite. The symmetry of these crystal structures directly impacts the band structure of materials. Various methods have been developed to optimize the band structure and transport properties through manipulating the crystal structure. Eleonora Isotta et al[55] demonstrated that the transition from an ordered to a disordered structure in Cu_2ZnSnS_4 improves the thermoelectric properties of materials, primarily due to alterations in the electronic band structure as shown in **Figure 5**. They found a second-order reversible phase transition occurring near 533K. **Figure 5a** shows that the *S* increases sharply around the transition temperature, attributed to the higher symmetry associated with the disordered structure. At the same time, the σ of the material dramatically drops at the phase transition temperature, as shown in **Figure 5b**. Through the electronic band calculation, they found that in disordered structures, the energy difference among the first three valence bands decrease, the top of the valence band flattens, and the band gap also decreases, as shown in the **Figure 5c**. Following this, Akira Nagaoka et al[56] employed a pseudo-cubic strategy to enhance the thermoelectric performance of Cu_2ZnSnS_4 single crystal, as shown in **Figure 6**. They obtained the degenerate electron energy bands in the pseudo-cubic structure, resulting

in a high *S* and a remarkable *ZT* value of 1.6 at 800K in the material.

In addition, several methods can effectively improve the *S* of materials without altering their band structure. For example, by introducing energy barriers at the interface through doping or incorporation of secondary phase, low-energy carriers would be greatly scattered while high-energy carriers can pass through, achieving the goal of improving *S*. Qiufan Chen et al[57] doped Ag atoms into $Cu_2CdSnSe_4$ using a chemical method, successfully embedding a disordered sphalerite structure within the ordered sphalerite phase. This modification caused the energy band at the interface to bend, thereby generating energy barriers that effectively scatter low-energy carriers. As a result, both the *S* and σ were improved. Jolly Jacob et al[58] adopted a similar strategy by doping Cd into Cu_2ZnSnS_4 and found that the *S* increased with adding Cd. They found that, Cd doping led to the formation of Cu-based secondary phases. These secondary phases serve as effective filters for low-energy carriers, while allowing only high-energy carriers to pass through, thereby improving the performance of material. Additionally, introducing spin entropy by doping magnetic particles such as Ni[59] or elements such as Pb and Te[60] can effectively increase the effective mass and improve the *S* of the material.

3 Optimization of Thermal Transport Performance

We know that the transfer of thermal energy is mainly achieved through lattice vibrations and carrier transport, with the former represented as lattice thermal conductivity κ_l and the latter as electronic thermal conductivity κ_e. They can be

represented as:

$$\kappa_l = \frac{1}{3} C_V \upsilon l \tag{5}$$

$$\kappa_e = L\sigma T \tag{6}$$

In the above equation, C_v is specific heat at constant volume of materials, υ is phonon velocity, l is mean free path of phonon collision[61], L is Lorentz constant. Although the complex crystal structure and elemental composition of Cu-based quaternary diamondoid materials result in relatively low intrinsic thermal conductivity, there is still room for further optimization. Unlike κ_e, κ_l is almost independent of other electronic transport parameters, and can be regulated independently. To this end, many researchers have focused on reducing the κ_l to improve the thermoelectric performance. Defect control and microstructure design are two effective methods for reducing κ_l.

3.1 Defect Control

Compared to C_v and υ, the l is easier to regulate, particularly through controlling the defects state in the material. So far, introducing appropriate defects into the lattice to reduce the l has remained the main strategy for suppressing κ_l. The impact of point defects mainly lies in the fluctuation of the mass field caused by different atomic masses and the fluctuation of the stress field caused by different atomic radii. The larger the difference, the stronger the scattering effect on high-frequency phonons, and the better the result in reducing κ_l. For example, Qiufan Chen et al[57] prepared Ag-doped $Cu_2CdSnSe_4$ using a chemical method, which introduced Ag_{Cu} point defects into the

matrix, distorting the crystal structure and enhancing the phonon scattering. In addition, Qingfeng Song et al[62] introduced excess Cu into $Cu_2MnSnSe_4$, increasing local lattice distortion and suppressing κ_l. Studies also indicate that replacing Zn with Co in $Cu_2ZnSnSe_4$ increases point defects, reduces phonon relaxation time, and thus decrease κ_l [63]. Besides, anionic substitution significantly reduces the κ_l of $Cu_2ZnGeSe_{4-x}S_x$[64], primarily due to the disorder caused by substitution. Ultra-low κ_l can also be achieved in the locally disordered $Cu_{2+x}Zn_{1-x}SnS_4$[43], which is mainly attributed to the highly disordered arrangement of Cu and Zn in the lattice, causing phonon localization and shortening the phonon mean free path. Some researchers also use lattice strain to regulate the thermoelectric properties of materials[65]. They introduce lattice strain by creating dislocations, which reduce the relaxation time of phonons and enhance their scattering, as shown in **Figure 7**.

3.2 Microstructure Design

In addition to introducing point defects, microstructure design, such as nano precipitate, nanocrystalline material, and secondary phase boundary, can also reduce κ_l. For example, Feng-Jia Fan et al[66] synthesized $Cu_2CdSnSe_4$ nanocrystals through colloidal synthesis and prepared bulk materials by hot pressing. In their work, the nanocrystals generated more grain boundaries, significantly enhancing phonon scattering. This ultimately resulted in a thermal conductivity of 1.7 W m^{-1} K^{-1}at room temperature, which is about 40% lower than that of the bulk sample prepared by solid-state reaction. After that, Kaya Wei et al[67] reported the preparation of nanostructured

$Cu_2ZnSnSe_4$ and $Ag_2ZnSnSe_4$, once again confirming the impact of nanomaterials on the κ_l of these materials. Combining bulk materials with nanocrystals can reduce thermal conductivity while maintaining the high electrical properties of the bulk material. Qiufan Chen et al[68] prepared $Cu_2CdSnSe_4$ nanocrystals using colloidal synthesis and added these nanocrystals into the $Cu_2CdSnSe_4$ matrix, as shown in **Figure 8**. They found that this hierarchical architecture is able to suppress the thermal conductivity while preserving the decent electrical properties. The increased grain boundaries and embedded nanocrystals significantly enhanced phonon scattering, especially the latter serving as additional scattering centers that effectively scatter medium to long wavelength phonons, thereby reducing κ_l. Himanshu Nautiyal et al[69] synthesized disordered nanostructured polycrystals of Cu_2ZnSnS_4 and $Cu_2ZnSnSe_4$ through high-energy reaction mechanical alloying, achieving a low thermal conductivity of 0.2 W m^{-1} K^{-1}. Similar studies have also been conducted by Binayak Mukherjee et al[70], who obtained cubic $Cu_2ZnSnSe_4$ nanostructures with a low thermal conductivity of 0.21W m^{-1} K^{-1}.

The optimization of thermal conductivity through grain boundary engineering through the introduction of a secondary phase has also been proven to be an effective method. The interface between the secondary phase and the matrix generates strong phonon scattering. Yingcai Zhu et al[71] replaced Sn with Pb in $Cu_2ZnSnSe_4$ and found that Pb primarily exists in the PbSe framework, distributed as a secondary phase at grain boundaries, as shown in **Figure 9**. The phase interface between the secondary phase and the matrix has a strong scattering effect on phonons. Additionally, the smaller grain

size of the secondary phase increases the density of grain boundaries and further reduces the κ_l. Furthermore, the composite of CdSe and $Cu_2CdSnSe_4$ forms a coherent phase interface, allowing charge carriers to pass through while scattering phonons across a wide frequency spectrum[72]. The Cd vaporization during the hot pressing, creating nanopores in the material that introduce additional scattering centers, significantly reducing the κ_l.

4 Summary and Outlook

Recently, diamondoid thermoelectric materials have gained significant attention due to their unique electronic and thermal transport properties. Although their thermoelectric performance has yet to reach the levels of traditional thermoelectric materials, they are still a new star with great research potential. This article focuses on Cu-based quaternary diamondoid materials and provides a collection of recent progress and a comprehensive view of the optimization strategies for improving their electrical and thermal properties. We have thoroughly discussed the influence of various defects on the carrier concentration, carrier mobility and the band structure of the Cu-based quaternary diamondoid materials. Additionally, we have summarized a series of effective methods to enhance the phonon scattering and suppress the thermal conductivity. Overall, improving the carrier mobility while further reducing the thermal conductivity is critical for achieving high thermoelectric performance in these materials. In this context, the recently proposed off-centering effect may offer a new perspective and provide promising pathways for future optimization. In summary, although

significant progress has been made in promoting the thermoelectric performance of these systems, many challenges remain unresolved. We hope this review provide fresh insights and sparks new ideas for further improving the thermoelectric performance of these promising materials.

Competing interests

The authors declare no competing interests.

Acknowledgements

This work was primarily supported by the National Natural Science Foundation of China (52471217), National Science Fund for Distinguished Young Scholars (51925101), National Natural Science Foundation of China (52450001, 52250090, 52371208, 52002042, 51772012, 51571007, and 12374023), the Beijing Natural Science Foundation (JO18004), and the 111 Project (B17002). L. D. Z. appreciates the support from the Tencent Xplorer Prize.

References

[1] Xie, H.,Zhao, L. D.,Kanatzidis, M. G., *Interdiscip. Mater.*, 2024, 3, 51.

[2] Liu, Y.,Xie, H.,Li, Z.,Zhang, Y.,Malliakas, C. D.,Al Malki, M.,Ribet, S.,Hao, S.,Pham, T.,Wang, Y.,Hu, X.,dos Reis, R.,Snyder, G. J.,Uher, C.,Wolverton, C.,Kanatzidis, M. G.,Dravid, V. P., *J. Am. Chem. Soc.*, 2023, 145, 8677.

[3] Xie, H. Y.,Su, X. L.,Hao, S. Q.,Wolverton, C.,Uher, C.,Tang, X. F.,Kanatzidis, M. G., *Phys. Rev. Mater.*, 2020, 4, 2.

[4] Zheng, Z.,Su, X. L.,Deng, R. G.,Stoumpos, C.,Xie, H. Y.,Liu, W.,Yan, Y. G.,Hao, S. Q.,Uher, C.,Wolverton, C.,Kanatzidis, M. G.,Tang, X. F., *J. Am. Chem. Soc.*, 2018, 140, 7.

[5] Xie, H. Y.,Zhao, L. D., *Mater. Futures*, 2024, 3, 1.

[6] Xie, H. Y.,Su, X. L.,Bailey, T. P.,Zhang, C.,Liu, W.,Uher, C.,Tang, X. F.,Kanatzidis, M. G., *Chem. Mater.*, 2020, 32, 6.

[7] Liu, D. R.,Wang, D. Y.,Hong, T.,Wang, Z. Y.,Wang, Y. P.,Qin, Y. X.,Su, L. Z.,Yang, T. Y.,Gao, X.,Ge, Z. H.,Qin, B. C.,Zhao, L. D., *Science*, 2023, 380, 6647.

[8] Zheng, Y.,Zhang, Q.,Su, X. L.,Xie, H. Y.,Shu, S. C.,Chen, T. L.,Tan, G. J.,Yan, Y. G.,Tang, X. F.,Uher, C.,Snyder, G. J., *Adv. Energy Mater.*, 2015, 5, 5.

[9] Gao, D. Z.,Wang, S. N.,Wen, Y.,Fang, F.,Li, Y. C.,Liu, S. B.,Wang, Y. K.,Xie, H. Y.,Qiu, Y. T.,Zhao, L. D., *Mater. Today Phys.*, 2024, 41.

[10] Xie, H.,Hao, S.,Bao, J.,Slade, T. J.,Snyder, G. J.,Wolverton, C.,Kanatzidis, M. G., *J. Am. Chem. Soc.*, 2020, 142, 955320.

[11] Zheng, G.,Su, X. L.,Xie, H. Y.,Shu, Y. J.,Liang, T.,She, X. Y.,Liu, W.,Yan, Y. G.,Zhang, Q. J.,Uher, C.,Kanatzidis, M. G.,Tang, X. F., *Energy Environ. Sci.*, 2017, 10, 12.

[12] He, J.,Tritt, T. M., *Science*, 2017, 357, 6358.

[13] Bai, S. L.,Zhang, X.,Zhao, L. D., *Acc. Chem. Res.*, 2023, 56, 21.

[14] Zhao, L. D.,Lo, S. H.,Zhang, Y. S.,Sun, H.,Tan, G. J.,Uher, C.,Wolverton, C.,Dravid, V. P.,Kanatzidis, M. G., *Nature*, 2014, 508, 7496.

[15] Zhao, L. D.,Tan, G. J.,Hao, S. Q.,He, J. Q.,Pei, Y. L.,Chi, H.,Wang, H.,Gong, S. K.,Xu, H. B.,Dravid, V. P.,Uher, C.,Snyder, G. J.,Wolverton, C.,Kanatzidis, M. G., *Science*, 2016, 351, 6269.

[16] Bozin, E. S.,Xie, H.,Abeykoon, A. M. M.,Everett, S. M.,Tucker, M. G.,Kanatzidis, M. G.,Billinge, S. J. L., *Phys. Rev. Lett.*, 2023, 131, 3.

[17] Qiu, J. H.,Yan, Y. G.,Luo, T. T.,Tang, K. C.,Yao, L.,Zhang, J.,Zhang, M.,Su, X. L.,Tan, G. J.,Xie, H. Y.,Kanatzidis, M. G.,Uher, C.,Tang, X. F., *Energy Environ. Sci.*, 2019, 12, 10.

[18] Zhu, B.,Liu, X. X.,Wang, Q.,Qiu, Y.,Shu, Z.,Guo, Z. T.,Tong, Y.,Cui, J.,Gu, M.,He, J. Q., *Energy Environ. Sci.*, 2020, 13, 7.

[19] Wang, L.,Wen, Y.,Bai, S. L.,Chang, C.,Li, Y. C.,Liu, S.,Liu, D. R.,Wang, S. Q.,Zhao, Z.,Zhan, S. P.,Cao, Q.,Gao, X.,Xie, H. Y.,Zhao, L. D., *Nat. Commun.*, 2024, 15, 1.

[20] Wang, S. Q.,Wen, Y.,Zhu, Y. C.,Wang, Z. Y.,Liu, D. R.,Zheng, J. Q.,Zhan, S. P.,Xie, H. Y.,Ge, Z. H.,Gao, X.,Cao, Q.,Chang, C.,Zhao, L. D., *Small*, 2024, 20, 202400866.

[21] Pang, H. M.,Qin, Y. X.,Qin, B. C.,Yu, L. X.,Su, X. L.,Liang, H.,Ge, Z. H.,Cao, Q.,Tan, Q.,Zhao, L. D., *Adv. Funct. Mater.*, 2024, 34, 202401716.

[22] Liu, S. B.,Wen, Y.,Bai, S. L.,Shi, H. A.,Qin, Y. X.,Qin, B. C.,Liu, D. R.,Cao, Q.,Gao, X.,Su, L. Z.,Chang, C.,Zhang, X.,Zhao, L. D., *Adv. Mater.*, 2024, 36, 25.

[23] Chen, X. X.,Wu, H. J.,Cui, J.,Xiao, Y.,Zhang, Y.,He, J. Q.,Chen, Y.,Cao, J.,Cai,

W.,Pennycook, S. J.,Liu, Z. H.,Zhao, L. D.,Sui, J. H., *Nano Energy*, 2018, 52, 246.

[24] Li, D.,Zhang, B. L.,Ming, H. W.,Wang, L.,Zu, Y.,Qin, X. Y., *ACS Appl. Mater. Interfaces*, 2021, 13, 29.

[25] Vinodhini, J.,Shalini, V.,Harish, S.,Ikeda, H.,Archana, J.,Navaneethan, M., *J. Colloid Interface Sci.*, 2023, 651, 436.

[26] Imasato, K.,Kang, S. D.,Ohno, S.,Snyder, G. J., *Mater. Horiz.*, 2018, 5, 1.

[27] Xie, H.,Liu, Y.,Zhang, Y.,Hao, S.,Li, Z.,Cheng, M.,Cai, S.,Snyder, G. J.,Wolverton, C.,Uher, C.,Dravid, V. P.,Kanatzidis, M. G., *J. Am. Chem. Soc.*, 2022, 144, 911320.

[28] Yu, J. J.,Fu, C. G.,Liu, Y. T.,Xia, K. Y.,Aydemir, U.,Chasapis, T. C.,Snyder, G. J.,Zhao, X. B.,Zhu, T. J., *Adv. Energy Mater.*, 2018, 8, 1.

[29] Cheng, X.,Zhu, B.,Yang, D.,Su, X.,Liu, W.,Xie, H.,Zheng, Y.,Tang, X., *ACS Appl. Mater. Interfaces*, 2022, 14, 54394.

[30] Hu, L.,Luo, Y. B.,Fang, Y. W.,Qin, F. Y.,Cao, X.,Xie, H. Y.,Liu, J. W.,Dong, J. F.,Sanson, A.,Giarola, M.,Tan, X. Y.,Zheng, Y.,Suwardi, A.,Huang, Y. Z.,Hippalgaonkar, K.,He, J. Q.,Zhang, W. Q.,Xu, J. W.,Yan, Q. Y.,Kanatzidis, M. G., *Adv. Energy Mater.*, 2021, 11, 42.

[31] Cheng, X.,Yang, D.,Su, X.,Xie, H.,Liu, W.,Zheng, Y.,Tang, X., *ACS Appl. Mater. Interfaces*, 2021, 13, 5517846.

[32] Cao, Y.,Su, X.,Meng, F.,Bailey, T. P.,Zhao, J.,Xie, H.,He, J.,Uher, C.,Tang, X., *Adv. Funct. Mater.*, 2020, 30, 51.

[33] Shi, X. Y.,Huang, F. Q.,Liu, M. L.,Chen, L. D., *Appl. Phys. Lett.*, 2009, 94, 12.

[34] Liu, M. L.,Chen, I. W.,Huang, F. Q.,Chen, L. D., *Adv. Mater.*, 2009, 21, 380837.

[35] Xie, H.,Hao, S.,Cai, S.,Bailey, T. P.,Uher, C.,Wolverton, C.,Dravid, V. P.,Kanatzidis, M. G.,

Energy Environ. Sci., 2020, 13, 369310.

[36] Liu, R. H.,Xi, L. L.,Liu, H. L.,Shi, X.,Zhang, W. Q.,Chen, L. D., *Chem. Commun.*, 2012, 48, 32.

[37] Plirdpring, T.,Kurosaki, K.,Kosuga, A.,Day, T.,Firdosy, S.,Ravi, V.,Snyder, G. J.,Harnwunggmoung, A.,Sugahara, T.,Ohishi, Y.,Muta, H.,Yamanaka, S., *Adv. Mater.*, 2012, 24, 27.

[38] Xie, H.,Li, Z.,Liu, Y.,Zhang, Y.,Uher, C.,Dravid, V. P.,Wolverton, C.,Kanatzidis, M. G., *J. Am. Chem. Soc.*, 2023, 145, 32115.

[39] Xie, H. Y.,Bozin, E. S.,Li, Z.,Abeykoon, M.,Banerjee, S.,Male, J. P.,Snyder, G. J.,Wolverton, C.,Billinge, S. J. L.,Kanatzidis, M. G., *Adv. Mater.*, 2022, 34, 24.

[40] Xie, H. Y.,Su, X. L.,Zheng, G.,Zhu, T.,Yin, K.,Yan, Y. G.,Uher, C.,Kanatzidis, M. G.,Tang, X. F., *Adv. Energy Mater.*, 2017, 7, 3.

[41] Xie, H. Y.,Su, X. L.,Hao, S. Q.,Zhang, C.,Zhang, Z. K.,Liu, W.,Yan, Y. G.,Wolverton, C.,Tang, X. F.,Kanatzidis, M. G., *J. Am. Chem. Soc.*, 2019, 141, 47.

[42] Liu, M.-L.,Huang, F.-Q.,Chen, L.-D.,Chen, I. W., *Appl. Phys. Lett.*, 2009, 94, 20.

[43] Jiang, Q.,Yan, H.,Lin, Y.,Shen, Y.,Yang, J.,Reece, M. J., *J. Mater. Chem. A*, 2020, 8, 1090921.

[44] Dong, Y.,Wang, H.,Nolas, G. S., *PHYS STATUS SOLIDI-R*, 2013, 8, 611.

[45] Li, Z.,Zhang, W.,Gu, B.,Zhao, C.,Ye, B.,Xiao, C.,Xie, Y., *J. Mater. Chem. A*, 2021, 9, 10062.

[46] Liu, F. S.,Zheng, J. X.,Huang, M. J.,He, L. P.,Ao, W. Q.,Pan, F.,Li, J. Q., *Sci. Rep.*, 2014, 4, 1.

[47] Wang, B.,Li, Y.,Zheng, J. X.,Xu, M.,Liu, F. S.,Ao, W. Q.,Li, J. Q.,Pan, F., *Sci. Rep.*, 2015,

5, 9365.

[48] Chetty, R.,Bali, A.,Mallik, R. C., *Intermetallics*, 2016, 72, 17.

[49] Mehmood, F.,Sun, Y.,Su, W.,Chebanova, G.,Zhai, J.,Wang, L.,Khan, M.,Romanenko, A.,Wang, H.,Wang, C., *PHYS STATUS SOLIDI-R*, 2022, 16, 6.

[50] Wei, K.,Beauchemin, L.,Wang, H.,Porter, W. D.,Martin, J.,Nolas, G. S., *J. Alloys Compd.*, 2015, 650, 844.

[51] Song, Q.,Qiu, P.,Chen, H.,Zhao, K.,Guan, M.,Zhou, Y.,Wei, T. R.,Ren, D.,Xi, L.,Yang, J.,Chen, Z.,Shi, X.,Chen, L., *Mater. Today Phys.*, 2018, 7, 45.

[52] Parashchuk, T.,Cherniushok, O.,Smitiukh, O.,Marchuk, O.,Wojciechowski, K. T., *Chem. Mater.*, 2023, 35, 477212.

[53] Sharma, S. D.,Bayikadi, K.,Raman, S.,Neeleshwar, S., *Nanotechnology*, 2020, 31, 36540236.

[54] Ashfaq, A.,Ali, A.,Mahmood, K.,Rehman, U. u.,Tahir, S.,Amin, N.,Ahmad, W.,Aslam, R. N.,Arshad, M.,Rasheed, K., *Ceram. Int.*, 2021, 47, 3535624.

[55] Isotta, E.,Fanciulli, C.,Pugno, N. M.,Scardi, P., *Nanomaterials*, 2019, 9, 7625.

[56] Nagaoka, A.,Yoshino, K.,Masuda, T.,Sparks, T. D.,Scarpulla, M. A.,Nishioka, K., *J. Mater. Chem. A*, 2021, 9, 1559528.

[57] Chen, Q. F.,Wang, G. W.,Zhang, A. J.,Yang, D. F.,Yao, W.,Peng, K. L.,Yan, Y. C.,Sun, X. N.,Liu, A. P.,Wang, G. Y.,Zhou, X. Y., *J. Mater. Chem. C*, 2015, 3, 47.

[58] Jacob, J.,Ali, H. T.,Ali, A.,Mehboob, K.,Ashfaq, A.,Ikram, S.,Rehman, U.,Mahmood, K.,Amin, N., *Mater. Sci. Semicond. Process.*, 2021, 123, 105587.

[59] Xiao, C.,Li, K.,Zhang, J. J.,Tong, W.,Liu, Y. W.,Li, Z.,Huang, P. C.,Pan, B. C.,Su, H. B.,Xie,

Y., *Mater. Horiz.*, 2014, 1, 1.

[60] Huo, T.,Mehmood, F.,Wang, H.,Su, W.,Wang, X.,Chen, T.,Zhang, K.,Feng, J.,Wang, C., *Phys. Status Solidi A*, 2020, 217, 17.

[61] Xie, H. Y.,Su, X. L.,Zhang, X. M.,Hao, S. Q.,Bailey, T. P.,Stoumpos, C. C.,Douvalis, A. P.,Hu, X. B.,Wolverton, C.,Dravid, V. P.,Uher, C.,Tang, X. F.,Kanatzidis, M. G., *J. Am. Chem. Soc.*, 2019, 141, 27.

[62] Song, Q.,Qiu, P.,Chen, H.,Zhao, K.,Ren, D.,Shi, X.,Chen, L., *ACS Appl. Mater. Interfaces*, 2018, 10, 1012312.

[63] Zhu, Y.,Liu, Y.,Ren, G.,Tan, X.,Yu, M.,Lin, Y.-H.,Nan, C.-W.,Marcelli, A.,Hu, T.,Xu, W., *Inorg. Chem.*, 2018, 57, 605110.

[64] Heinrich, C. P.,Day, T. W.,Zeier, W. G.,Snyder, G. J.,Tremel, W., *J. Am. Chem. Soc.*, 2013, 136, 4421.

[65] Sun, Y.,Abbas, A.,Wang, H.,Tan, C.,Li, Z.,Zong, Y.,Sun, H.,Wang, C.,Wang, H., *Chem. Eng. J.*, 2024, 486, 150158.

[66] Fan, F.-J.,Yu, B.,Wang, Y.-X.,Zhu, Y.-L.,Liu, X.-J.,Yu, S.-H.,Ren, Z., *J. Am. Chem. Soc.*, 2011, 133, 1591040.

[67] Wei, K.,Nolas, G. S., *ACS Appl. Mater. Interfaces*, 2015, 7, 975218.

[68] Chen, Q.,Yan, Y.,Zhan, H.,Yao, W.,Chen, Y.,Dai, J.,Sun, X.,Zhou, X., *J. Materiomics*, 2016, 2, 1792.

[69] Nautiyal, H.,Lohani, K.,Mukherjee, B.,Isotta, E.,Malagutti, M. A.,Ataollahi, N.,Pallecchi, I.,Putti, M.,Misture, S. T.,Rebuffi, L.,Scardi, P., *Nanomaterials*, 2023, 13, 3662.

[70] Mukherjee, B.,Isotta, E.,Malagutti, M. A.,Lohani, K.,Rebuffi, L.,Fanciulli, C.,Scardi, P., *J.*

Alloys Compd., 2023, 933, 167756.

[71] Zhu, Y.,Liu, Y.,Tan, X.,Ren, G.,Yu, M.,Hu, T.,Marcelli, A.,Xu, W., *AIP Adv.*, 2018, 8, 4.

[72] Basu, R.,Mandava, S.,Bohra, A.,Bhattacharya, S.,Bhatt, R.,Ahmad, S.,Bhattacharyya, K.,Samanta, S.,Debnath, A. K.,Singh, A.,Aswal, D. K.,Muthe, K. P.,Gadkari, S. C., *J. Electron. Mater.*, 2019, 48, 4.

[73] El Hamdaoui, J. E.,Kria, M.,Lakaal, K.,El-Yadri, M.,Feddi, E. M.,Pedraja Rejas, L. P.,Pérez, L. M.,Díaz, P.,Mora-Ramos, M. E.,Laroze, D., *Int. J. Mol. Sci.*, 2022, 23, 1278521.

[74] Zeier, W. G.,LaLonde, A.,Gibbs, Z. M.,Heinrich, C. P.,Panthöfer, M.,Snyder, G. J.,Tremel, W., *J. Am. Chem. Soc.*, 2012, 134, 16.

[75] Kumar, V. P.,Guilmeau, E.,Raveau, B.,Caignaert, V.,Varadaraju, U. V., *Journal of Applied Physics*, 2015, 118, 15.

[76] Chetty, R.,Dadda, J.,de Boor, J.,Müller, E.,Mallik, R. C., *Intermetallics*, 2015, 57, 156.

[77] Ibáñez, M.,Zamani, R.,LaLonde, A.,Cadavid, D.,Li, W. H.,Shavel, A.,Arbiol, J.,Morante, J. R.,Gorsse, S.,Snyder, G. J.,Cabot, A., *Journal of the American Chemical Society*, 2012, 134, 9.

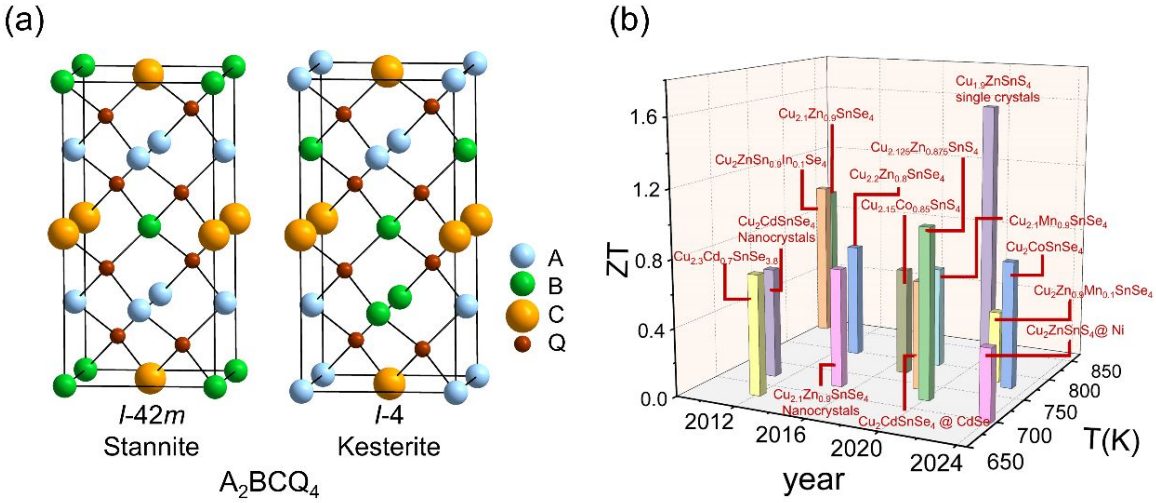

Figure 1 The development of quaternary diamondoid thermoelectric materials. (a) Structure of quaternary diamondoid thermoelectric materials. (b) Current state of the art quaternary diamondoid thermoelectric materials, the figure - of - merit *ZT* as a function of temperature and the published time.

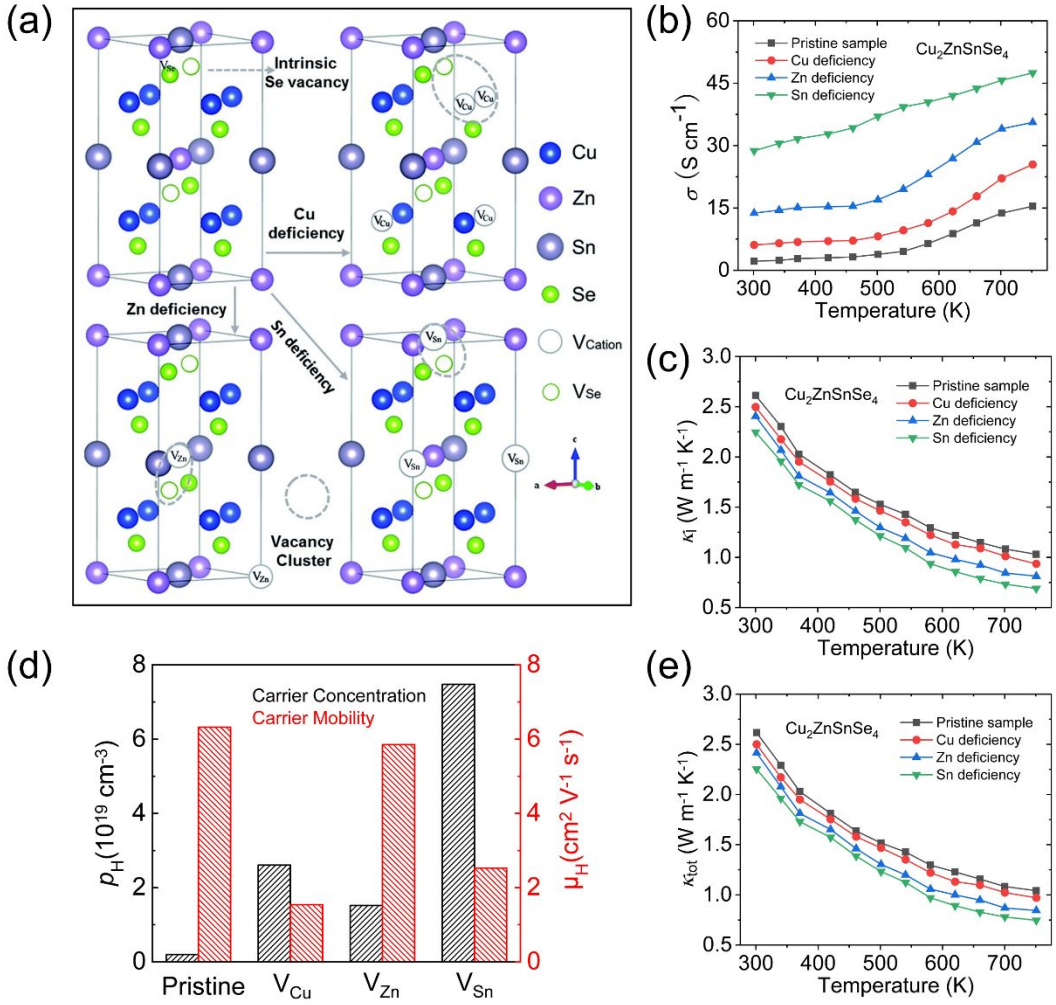

Figure 2 The influence of different cation vacancies on thermoelectric transport properties for $Cu_2ZnSnSe_4$. (a) Schematic diagram of different cation vacancies in $Cu_2ZnSnSe_4$. Temperature dependence of (b) Electric conductivity (σ) and (c) Lattice thermal conductivity (κ_l). (d) The room temperature of carrier concentration (p_H) and mobility(μ_H) for different samples. (e) Total thermal conductivity (κ_{tot}) as a function of temperature.

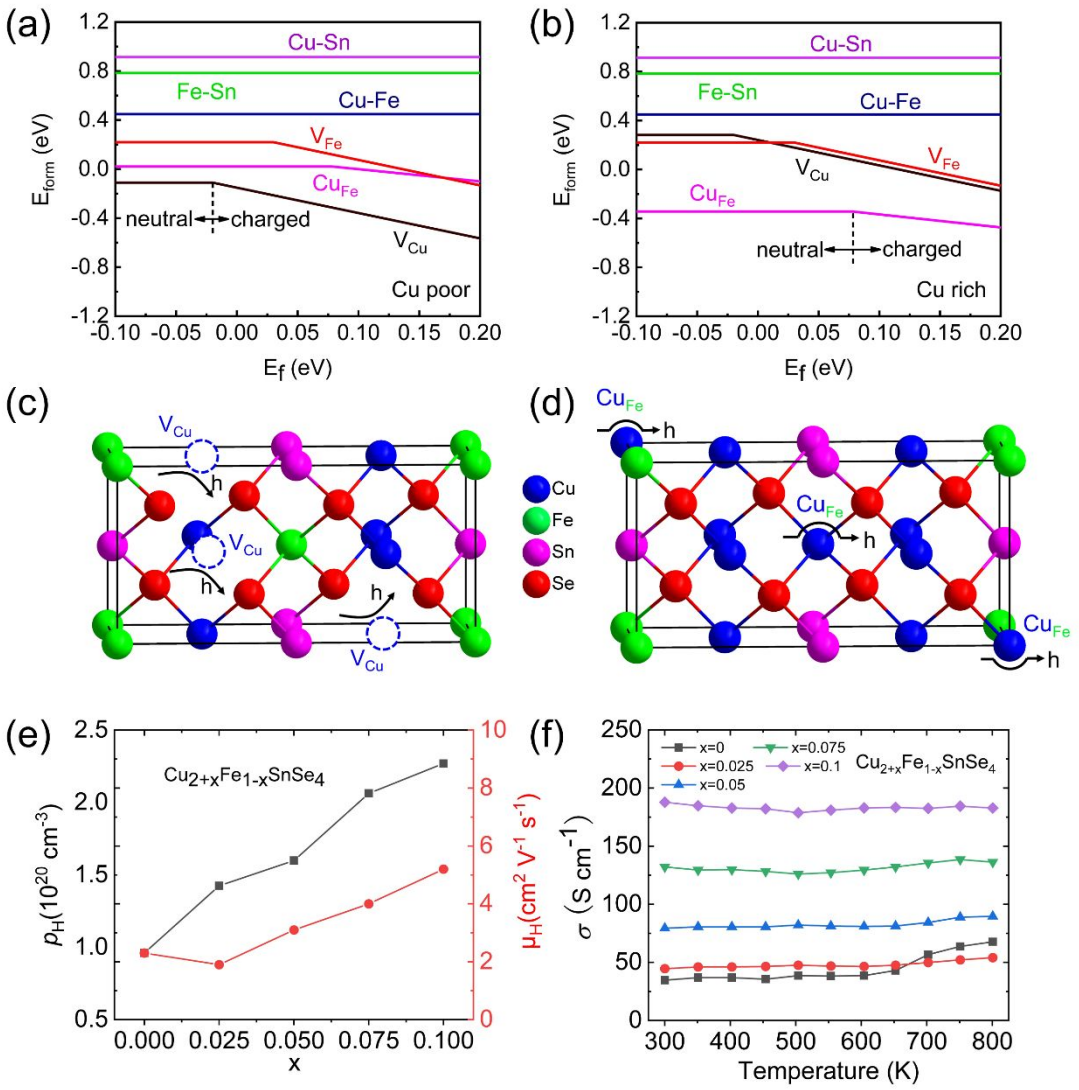

Figure 3 The influence of different defects on carrier transport in $Cu_2FeSnSe_4$. (a) Defect formation energy of Cu-poor conditions. (b) Defect formation energy of Cu-rich conditions. Schematic diagram of charge carriers scattering by (c) V_{Cu} vacancy and (d) Cu_{Fe} anti-site defect. (e) The room temperature carrier concentration (p_H) and mobility (μ_H) for $Cu_{2+x}Fe_{1-x}SnSe_4$. (f) Electric conductivity (σ) as a function of temperature for $Cu_{2+x}Fe_{1-x}SnSe_4$.

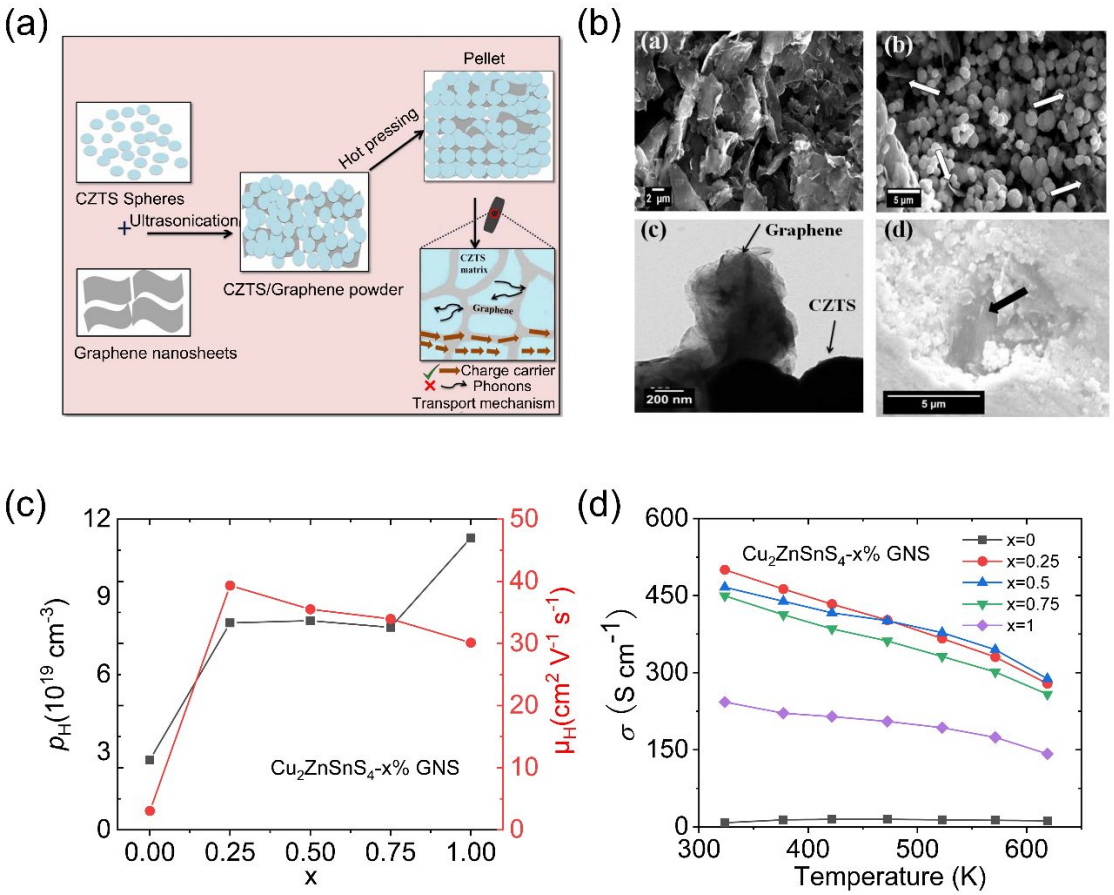

Figure 4 Introducing graphene to improve the electrical transport performance of Cu_2ZnSnS_4. (a) Schematic diagram shows the microstructure of sample. (b) SEM micrographs and TEM image of Cu_2ZnSnS_4/0.75 wt% GNs composite powder. (c) The room temperature carrier concentration (p_H) and mobility (μ_H) of graphene doped samples. (d) Temperature dependence of electric conductivity (σ).

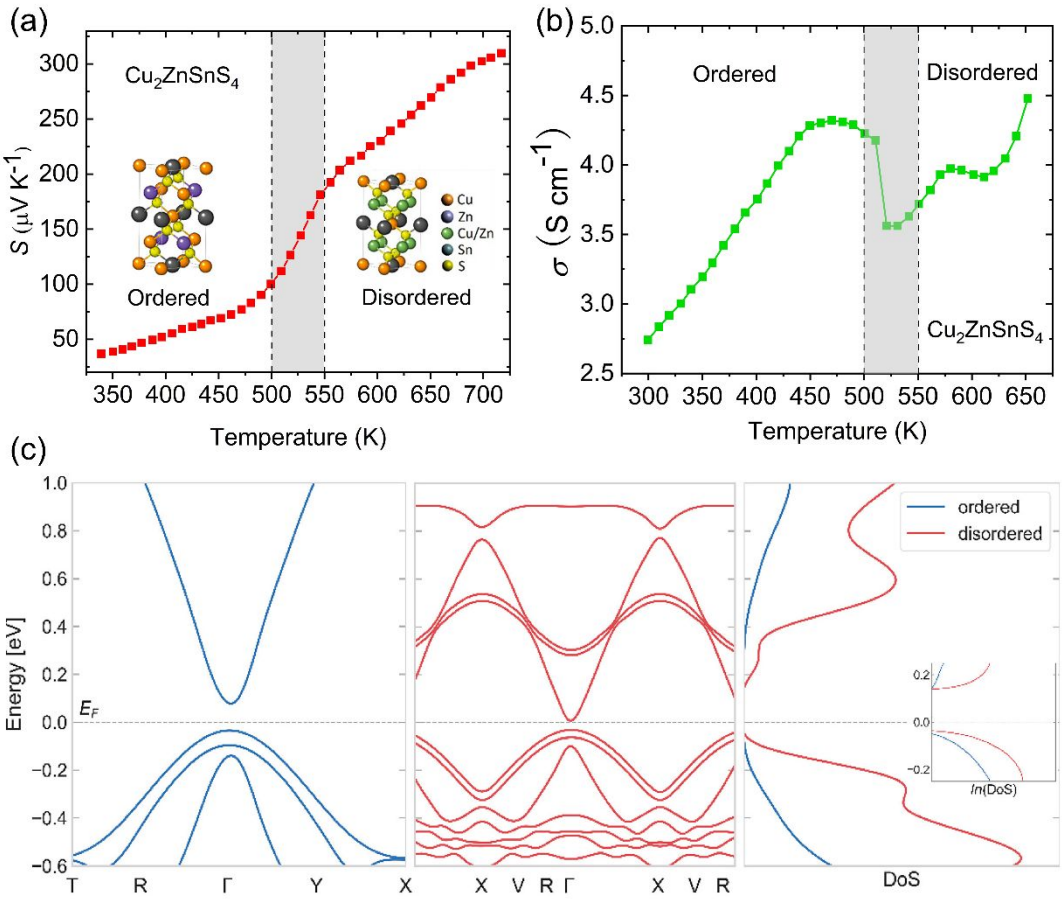

Figure 5 The influence of ordered and disordered structure on electrical transport performance of Cu_2ZnSnS_4. Temperature dependence of (a) Seebeck coefficient (S) and (b) electric conductivity (σ). (c) The band structures and density of states for ordered and disordered Cu_2ZnSnS_4.

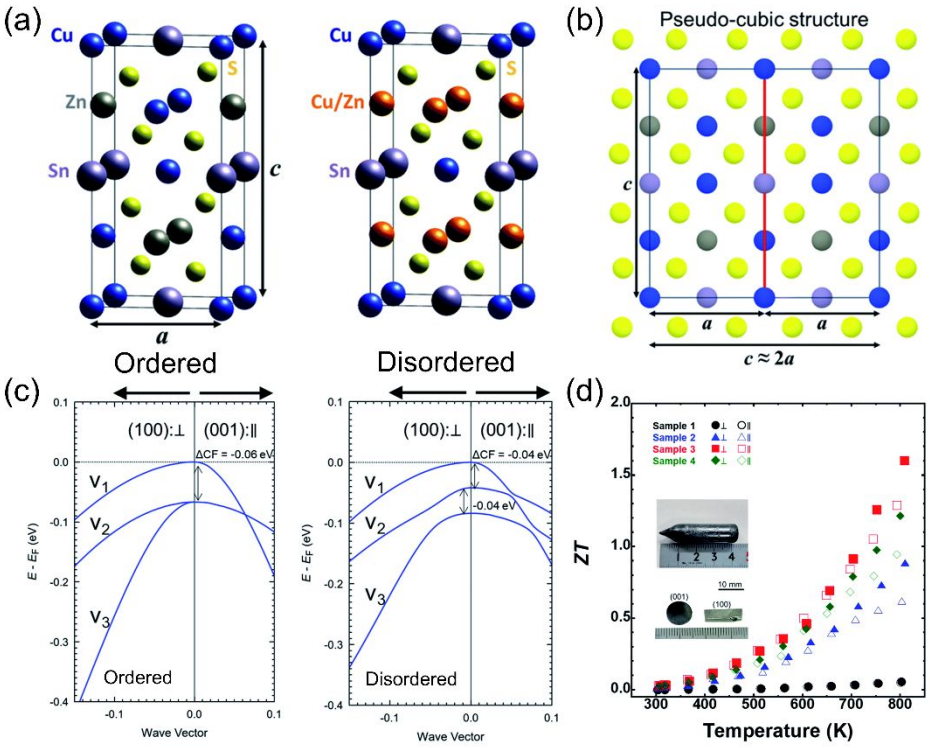

Figure 6 The crystal structure and transport properties of Cu_2ZnSnS_4. (a) The crystal structures of ordered and disordered Cu_2ZnSnS_4. (b) Pseudo-cubic structure shows the crystal structure parameter η (c/2a) ≈ 1. (c) The valence bands for the ordered and disordered Cu_2ZnSnS_4. (d) Temperature dependence of *ZT* for Cu_2ZnSnS_4 single crystals with different composition.

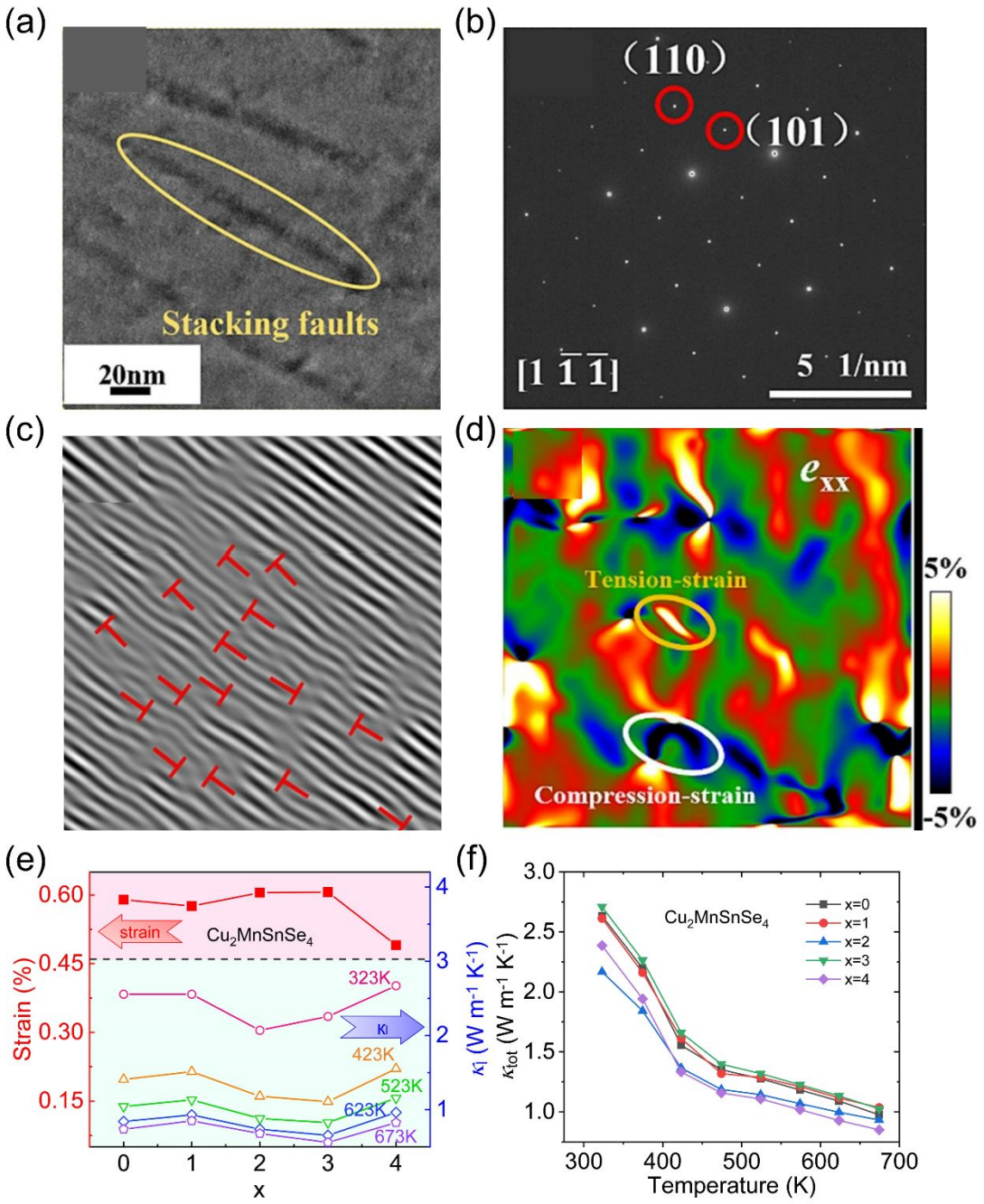

Figure 7 The influence of lattice strain on thermal conductivity. (a) The TEM image of $Cu_2MnSnSe_4$ showing the stacking faults in the matrix. (b) SAED pattern of $Cu_2MnSnSe_4$ along [1 -1 -1] direction. (c) The IFFT image showing dislocation in the material. (d) The corresponding strain mapping of $Cu_2MnSnSe_4$ lattice. (e) The lattice thermal conductivity (κ_l) and lattice strain of $Cu_2MnSnSe_4$. (f) Temperature dependence of total thermal conductivity (κ_{tot}) of $Cu_2MnSnSe_4$.

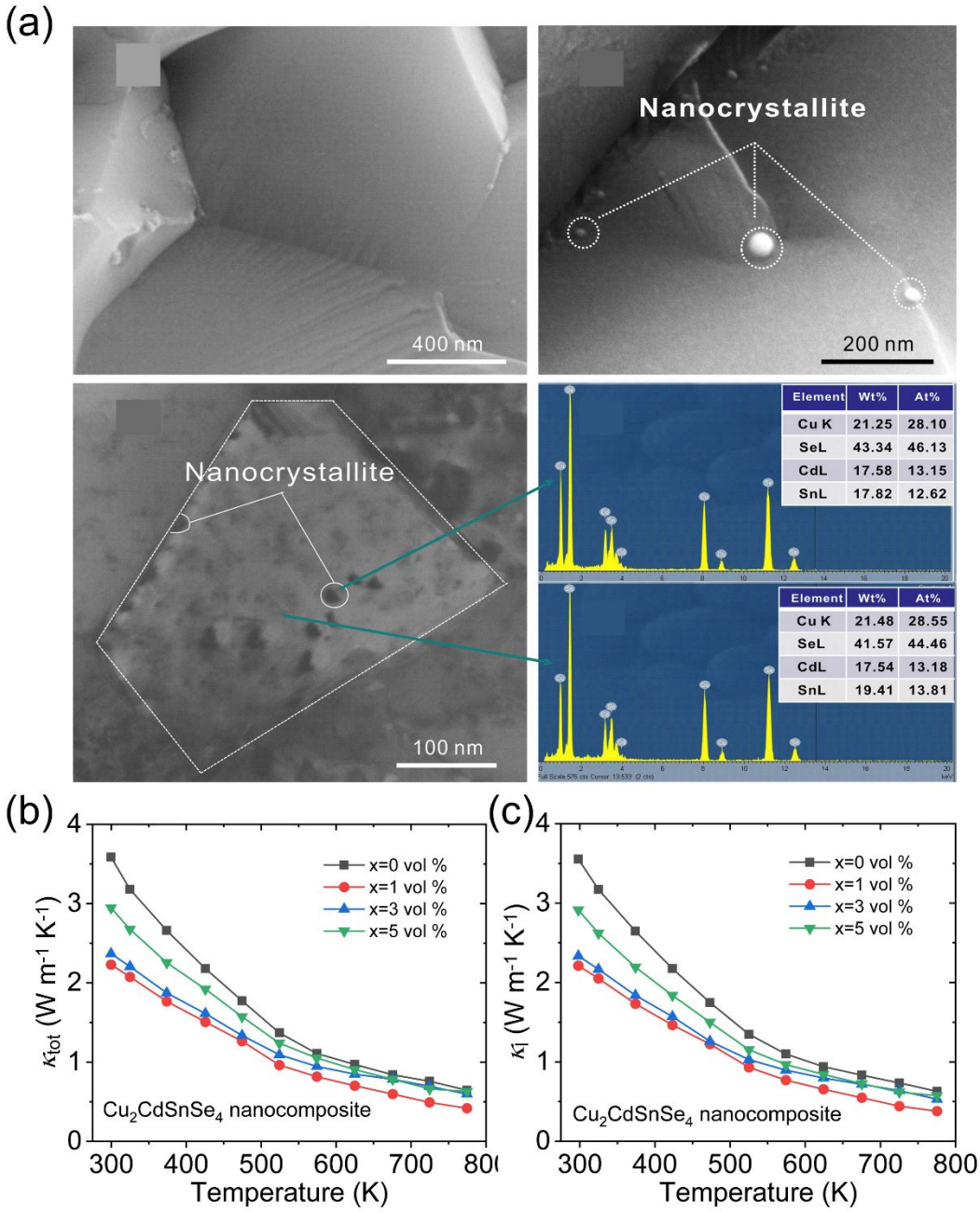

Figure 8 Morphology and thermal properties of nanocomposite materials. (a) The morphology of fracture surface for $Cu_2CdSnSe_4$ matrix and the nanocomposite. Temperature dependence of (b) total thermal conductivity (κ_{tot}) and (c) lattice thermal conductivity (κ_l) for $Cu_2CdSnSe_4$ nanocomposite materials.

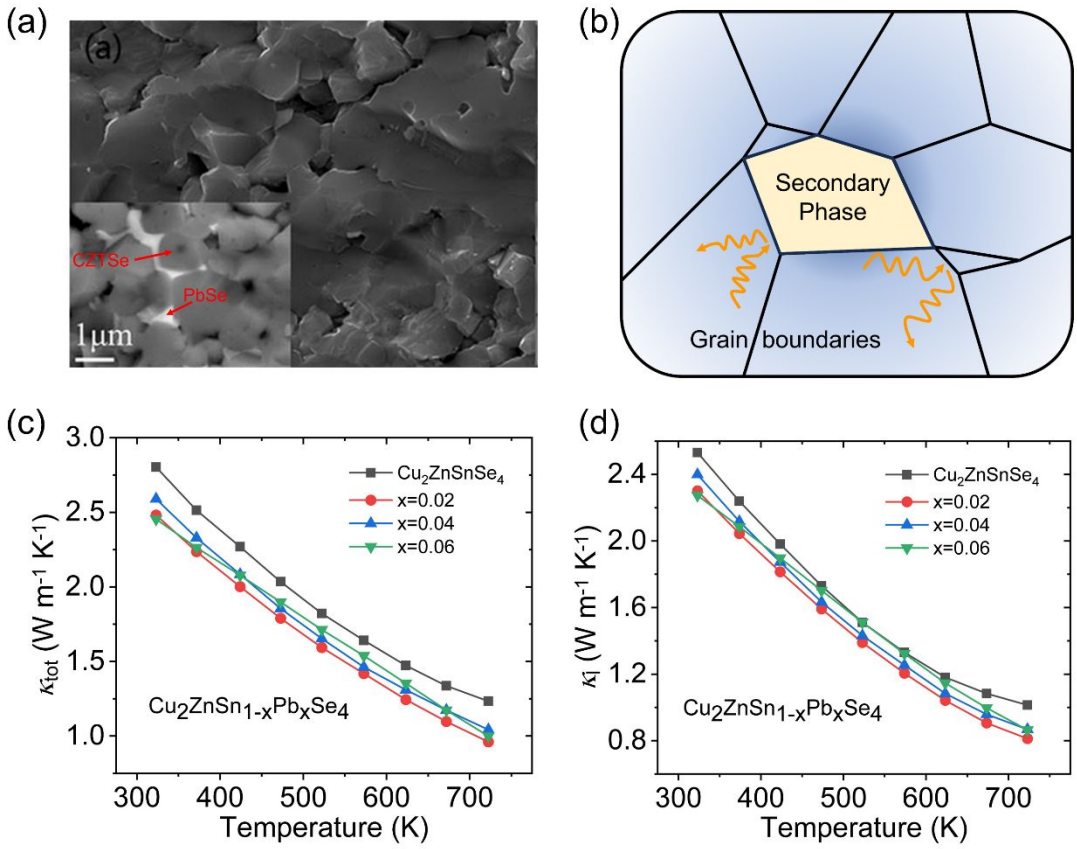

Figure 9 The structure and thermal properties of $Cu_2ZnSn_{1-x}Pb_xSe_4$. (a) SEM image of $Cu_2ZnSn_{1-x}Pb_xSe_4$. (b) Schematic diagram of secondary phase boundary scattering. Temperature dependence of (c) total thermal conductivity (κ_{tot}) and (d) lattice thermal conductivity (κ_l) of $Cu_2ZnSn_{1-x}Pb_xSe_4$.

Table1 Space group,band gap and *ZT* of Cu-based quaternary diamondoid compounds

Chemical formula	Space group	E_g (eV)	*ZT*, T(K)	Ref.
Cu_2ZnSnS_4	I-42m	1.4	0.36, 700	[42]
Cu_2ZnGeS_4	I-42m	2.05	/	[73]
$Cu_2ZnSnSe_4$	I-42m	1.41	0.95, 850	[42]
$Cu_2CdSnSe_4$	I-42m	0.96	0.65, 700	[34]
$Cu_2HgSnSe_4$	I-42m	1.81	0.2, 723	[74]
$Cu_2MgSnSe_4$	I-42m	1.7	0.42, 700	[75]
$Cu_2CdGeSe_4$	I-42m	1.2	0.42, 723	[76]
$Cu_2ZnGeSe_4$	I-42m	1.4	0.55, 723	[77]

Recent Progress on Quaternary Copper-based Diamondoid Thermoelectric Materials

Zihao Zhao[1], Hongyao Xie[1,*], Li-Dong Zhao[1,*]

[1]*School of Materials Science and Engineering, Beihang University, Beijing 100191, China.*

E-mail: xiehongyao@buaa.edu.cn; *zhaolidong@buaa.edu.cn*

Abstract: The rising concern on energy and environmental crises have sparked global interest in developing sustainable new energy and high-efficient energy conversion technologies. Thermoelectric technology has gained attention due to its potential for application in waste heat recovery and solid-state refrigeration. However, the application of traditional thermoelectric materials remains limited due to their expensive and toxic elemental composition. Recently, quaternary copper-based diamondoid materials have garnered significant interest due to their unique transport properties, high element abundance, and low toxicity. Many of these materials have demonstrated promising *ZT* value, positioning them as potential candidates for efficient thermoelectric applications. This paper summarizes the recent progress in copper-based quaternary diamondoid materials. We present a collection of research focused on optimizing electrical transport properties through carrier concentration tuning and band engineering, along with an overview of reducing thermal conductivity *via* microstructure enhanced phonon scattering. Finally, we analyze the current research bottlenecks in copper-based quaternary diamondoid thermoelectric materials and propose future research directions.

Keywords: quaternary Cu-based diamondoid materials, thermoelectric performance, carrier concentration, band engineering, microstructure

1 Introduction

The continuous rise in global energy demand and the depletion of unrenewable fossil fuels have made the development of sustainable new energy and high-efficiency energy conversion technologies become the worldwide topics. Research indicates that approximately 65% of energy produced in human activities is wasted and lost as heat[1]. Thus, developing effective methods to recovery this waste heat is considered as a way to solve the energy problems. Thermoelectric materials[2-4], based on the Seebeck effect, can directly convert heat into electricity, and can also be used for solid state cooling. This makes them a promising tool for mitigating energy crises[5]. However, the low energy conversion efficiency of thermoelectric materials limits their large-scale commercial applications[6].

Generally, the performance of thermoelectric materials is mainly evaluated by the dimensionless thermoelectric figure of merit ZT, $ZT = S^2\sigma T / \kappa_{tot} = S^2\sigma T / (\kappa_e + \kappa_l)$, where S is Seebeck coefficient, σ is electrical conductivity, T is absolute temperature, κ_e is electronic thermal conductivity, κ_l is lattice thermal conductivity, and the sum of κ_e and κ_l is the total thermal conductivity of the material κ_{tot}[7-9]. $PF = S^2\sigma$, which is a power factor used to characterize the electrical transport performance of thermoelectric materials. Therefore, to improve the performance of thermoelectric materials, two main approaches are typically pursued: (1) optimizing the electrical properties; (2) reducing thermal conductivity[10, 11]. However, because of the strong inherent coupling between electrical conductivity σ, Seebeck coefficient S, and thermal conductivity κ_{tot}, it is challenging to solely regulate these parameters to achieve high

thermoelectric performance[12]. For instance, increasing the carrier concentration can enhance σ, but this often reduces the S and increases κ_e, limiting the overall improvement in ZT. To overcome this, researchers employ various strategies to decouple these properties, aiming for enhanced thermoelectric efficiency.

Since the discovery of thermoelectric effect, researchers have identified numerous high-performance thermoelectric materials. For example, SnQ (Q= S, Se)[13-16], Bi_2Te_3 alloy[8, 11, 17, 18], PbQ (Q=S, Se, Te)[19-22], Zintl phase[23], Ag_2Q (Q=S, Se, Te)[24, 25], Mg_3X_2 (X=Sb, Bi)[26, 27] , half Heusler[28], and most recently, the diamondoid compound[29-32]. Early research on diamondoid compounds primarily concentrated on their optoelectronic properties, and their thermoelectric properties did not receive sufficient attention. Until the excellent thermoelectric properties of $Cu_2ZnSnSe_4$ and $Cu_2CdSnSe_4$ were first reported by Shi[33] and Liu et al[34]. In 2009, diamondoid thermoelectric materials have attracted widespread attention from the research community. Since then, a growing number of wide bandgap diamond-like materials have been reported, such as $CuInTe_2$, $CuGaTe_2$, $CuFeS_2$, Cu_2SnSe_3, Cu_3SbSe_4, etc[30, 35-41]. These materials derive from the sphalerite structure and has the typical tetrahedral coordination geometry of diamond. This stable twisted tetrahedral structure is formed by the "cross substitution" of element, following the "eight electron rule". Since the differences in electronegativity and radius between various anions and cations, phonon scattering in this twisted lattice is greatly enhanced, resulting in low κ_l. This characteristic is important for its decent thermoelectric performance. Quaternary Cu-based diamondoid materials generally have a chemical formula of A_2BCQ_4, with a

tetragonal lattice structure that exhibits a double-periodic cubic sphalerite structure along the z-direction, as shown in **Figure 1**. This complex crystal structure and elemental composition result in inherently low κ_l. In addition, the diverse elemental composition provides it a broad scope to tune the band structure and electrical properties through chemical composition regulation. However, compared to the ternary diamondoid materials, the *ZT* value of A_2BCQ_4 compounds is lower, typically not exceeding 1.0, mainly due to their lower intrinsic σ. Therefore, a large amount of research aims to improve the electrical properties of quaternary diamondoid materials. Among these materials, Cu-based quaternary diamondoid materials have garnered the most attention. In the next, we start with introducing the recent progress in improving the electronic properties of these materials.

2 Optimization of Electrical Transport Performance

Improving the electrical properties is vital for promoting the thermoelectric performance of quaternary diamondoid materials. However, there is a strong coupling between their σ and *S*, these parameters are closely related to the carrier concentration and effective mass of the material. The σ is directly proportional to the carrier concentration and mobility:

$$\sigma = en\mu \tag{1}$$

$$n = 4\pi\left(\frac{2m^* k_B T}{h^2}\right)^{\frac{3}{2}} F_{\frac{1}{2}}(\eta) \tag{2}$$

$$\mu = \frac{2e}{3m^*}\tau_0(\lambda+1)(k_B T)^{\lambda-\frac{1}{2}}\frac{F_\lambda(\eta)}{F_{1/2}(\eta)} \tag{3}$$

Among formulas, n is carrier concentration, μ is carrier mobility, $m^*$is effective mass of charge carrier, k_B is Boltzmann constant, h is planck constant, η is simplified Fermi level, τ_0 is relaxation time, λ is scattering factor. Based on the single parabolic band model and the relaxation time approximation, S can be derived from the following equation:

$$S = \frac{8\pi^2 k_B^2 T}{3eh^2} m^* \left(\frac{\pi}{3n}\right)^{\frac{2}{3}} \quad (4)$$

From equations 1 to 4, we can see that optimizing carrier concentration by doping and adjusting the Fermi level can significantly enhance σ. Additionally, modifying the density of states by adjusting the band structure and effective mass plays a crucial role in improving the S.

2.1 Optimization of Carrier Concentration

Optimizing the carrier concentration is one of the most direct methods to enhance electrical performance. The carrier concentration in a material is influenced by its defect states. Therefore, element doping is a common way to adjust the carrier concentration. Unlike traditional narrow bandgap thermoelectrics ($E_g \leq 0.5$ eV), most of Cu-based diamondoid thermoelectric materials exhibit relatively wide bandgaps, $E_g > 1$eV, as shown in **Table1**. Because of the wide bandgap, most diamondoid materials have intrinsic low carrier concentrations, and element doping is a common and useful method to increase their carrier concentrations and σ.

Recently, many researchers have attempted various doping methods in quaternary

diamondoid materials. According to the doping elements, they can be divided into intrinsic and extrinsic doping. Intrinsic doping or self-doping, occurs without introducing any other extrinsic elements, and achieve doping effect by regulating the stoichiometric ratio of the material. In Cu-based diamondoid materials, the predominant charge carriers responsible for electrical transport are holes. Given that the formation energy of copper vacancies is relatively small, these vacancies serve as intrinsic defects significantly influencing the electrical properties of the material. In the early report by Liu et al in 2009 on $Cu_2CdSnSe_4$[34], substituting Cd with Cu can effectively improve the σ. They found the [Cu_2Se_4] tetrahedral slabs function as electrically conducting units, while the [$SnCdSe_4$] units act as the electrically insulating structures. Thus, introducing excess Cu can not only introduce more intrinsic copper vacancies, generating more holes, but the insulating paths are also transformed into conductive ones due to the replacement of Cd with Cu. As a result, the σ of $Cu_{2.1}Cd_{0.9}SnSe_4$ achieved an impressive value of 20300 $S \cdot m^{-1}$ at room temperature, which is about six times higher than that of the pristine sample. The same strategy was successfully applied in another work in 2009[42], where excess Cu was introduced into $Cu_2ZnSnSe_4$. This result in an impressive σ of 86000 $S \cdot m^{-1}$ and achieved a groundbreaking ZT of 0.91 at 860K. Following these findings, many researchers adopted this strategy to improve the thermoelectric performance of diamondoid materials. For example, Qinghui Jiang et al[43] prepared Cu_2ZnSnS_4 samples using ball milling and hot press methods, and introduced additional Cu into the Zn sites to generate more hole carriers and improve σ. Finally, a high ZT value of 1.1 has been achieved for $Cu_{2.125}Zn_{0.875}SnS_4$.

Besides, Yongkwan Dong et al[44] explored introducing larger doses of Cu to further improve the σ of the material. Although introducing more low-valence cations at high valence sites has been proven to be an effective means of improving σ, excessive doping can easily lead to the formation of secondary phases. To address this, Zhou Li et al[45] explored optimizing the carrier concentration by constructing different cation vacancies in $Cu_2ZnSnSe_4$, as shown in **Figure 2**. They studied the effects of three types of cationic vacancies, Cu, Zn, and Sn, on electrical properties, and found that all samples exhibited a significant increase in hole concentration compared to the pristine samples. Notably, the Sn-deficient sample achieved the highest carrier concentration of 7.5×10^{19} cm^{-3}, resulting in an σ of 4700 $S\cdot m^{-1}$.

In addition to intrinsic doping, introducing extrinsic elements to increase the carrier concentration is a commonly used and effective optimization method. For example, X. Y. Shi et al[33] attempted to dope In at Sn site in $Cu_2ZnSnSe_4$, achieving a high carrier concentration that significantly improved the σ of the material, resulting in a record high *ZT* of 0.95 at 850K. Similarly, F. S. Liu et al[46] explored the role of doping Mn at Cd site in $Cu_2CdSnSe_4$ through experiment and theoretical calculation. They found that Mn doping causes the Fermi level to shift towards the valence band, resulting in a higher hole concentration while the carrier mobility decreases with increasing Mn content, ultimately leading to an increase in σ. Bo Wang et al[47] also achieved a similar effect by doping Ga at the Sn site in $Cu_2CdSnSe_4$. This strategy was also used in $Cu_2CdSn_{0.9}In_{0.1}Se_4$[48], $Cu_2MnSn_{0.95}In_{0.05}Se_4$[49] and $Cu_2ZnSn_{0.95}Ga_{0.05}Se_4$[50], further demonstrating the effectiveness of extrinsic doping in enhancing the thermoelectric

performance of quaternary diamondoid materials.

2.2 Optimization of Carrier Mobility

It is well known that, the carrier mobility of a material is closely related to the effective mass and scattering mechanisms. Therefore, a large amount of research on carrier mobility optimization has focused on these aspects. For example, Q. Song et al[51] optimized the lower intrinsic mobility of materials by manipulating the intrinsic lattice defects in $Cu_2FeSnSe_4$. They calculated the defect formation energies under both Cu-poor and Cu-rich conditions and identified the dominated defect types in $Cu_2FeSnSe_4$. In the case of Cu deficiency (**Figure 3a**), the defect formation energy of Cu vacancies is negative, indicating that Cu vacancies spontaneously occur during material preparation. Since the Cu vacancy is electronegative, making them to disrupt the original periodicity of the lattice and introduce additional ionized impurity scattering centers, thus reducing the carrier mobility, as shown in **Figure 3c**.

In contrast, they found that under Cu-rich condition, the defect formation energy of Cu atoms occupying Fe sites (Cu_{Fe} anti-site defect) is lower than that of Cu vacancies, indicating the Cu_{Fe} anti-site defect is dominant, as shown in **Figure 3b**. This defect is almost electrically neutral, so it causes only minimal disruption to the charge transport (**Figure 3d**). As a result, carrier mobility is less affected by scattering. Through carefully controlling the Cu content, they successfully achieved a synergistic optimization of both carrier mobility and carrier concentration, as shown in **Figure 3e**. And ultimately, it increased the conductivity of the material by about 2.5 times, as

shown in **Figure 3f**. Furthermore, doping In into $Cu_2MnSnSe_4$ can also improve the carrier mobility of the material[49]. This enhancement may be attributed to the optimization of band structure. In addition, by studying the transport properties of $Cu_2CoSnSe_4$ and Cu_2CoSnS_4. Taras Parashchuk et al[52] found that the selenide compound exhibited higher symmetry than its sulfide analogue, featuring with the bond angles closer to the ideal tetrahedral angle of 109.5°, this contribute to a higher carrier mobility.

Improving the electrical transport properties by introducing a secondary phase is a novel method. For example, Sarita Devi Sharma et al[53] improved the thermoelectric properties of Cu_2ZnSnS_4 by adding graphene nanosheets (GNs) into the matrix, as shown in **Figure 4**. The increase in σ is attributed to the formation of percolation channels created by the 2D graphene, which facilitates the transport of charge carriers. In this case, even small amount of GNs can produce a significant percolation effect. Additionally, the graphene nanosheets can exhibit a doping effect and moderately increase the carrier concentrations of the material.

Similarly, Arslan Ashfaq et al[54] prepared a series of Al-doped Cu_2ZnSnS_4 nanoparticles using the hydrothermal method, and found the extra Al effectively increases the σ of the material. This is because a small amount of Al particles diffuses into the gap of the matrix, forming bridge that allow charge carriers to pass freely through the grain boundaries, thus, increase the carrier concentration and mobility simultaneously.

2.3 Optimization of Seebeck Coefficient

The *S* is closely related to the density of states effective mass and carrier concentration. Although reducing carrier concentration is able to increase the *S*, it simultaneously lowers the σ. Therefore, band structure optimization emerges as a practical option to boost the *S* without compromising the σ. Cu-based quaternary diamondoid materials can exhibit two distinct crystal structures, the highly ordered Stannite and the disordered Kesterite. The symmetry of these crystal structures directly impacts the band structure of materials. Various methods have been developed to optimize the band structure and transport properties through manipulating the crystal structure. Eleonora Isotta et al[55] demonstrated that the transition from an ordered to a disordered structure in Cu_2ZnSnS_4 improves the thermoelectric properties of materials, primarily due to alterations in the electronic band structure as shown in **Figure 5**. They found a second-order reversible phase transition occurring near 533K. **Figure 5a** shows that the *S* increases sharply around the transition temperature, attributed to the higher symmetry associated with the disordered structure. At the same time, the σ of the material dramatically drops at the phase transition temperature, as shown in **Figure 5b**. Through the electronic band calculation, they found that in disordered structures, the energy difference among the first three valence bands decrease, the top of the valence band flattens, and the band gap also decreases, as shown in the **Figure 5c**. Following this, Akira Nagaoka et al[56] employed a pseudo-cubic strategy to enhance the thermoelectric performance of Cu_2ZnSnS_4 single crystal, as shown in **Figure 6**. They obtained the degenerate electron energy bands in the pseudo-cubic structure, resulting

in a high *S* and a remarkable *ZT* value of 1.6 at 800K in the material.

In addition, several methods can effectively improve the *S* of materials without altering their band structure. For example, by introducing energy barriers at the interface through doping or incorporation of secondary phase, low-energy carriers would be greatly scattered while high-energy carriers can pass through, achieving the goal of improving *S*. Qiufan Chen et al[57] doped Ag atoms into $Cu_2CdSnSe_4$ using a chemical method, successfully embedding a disordered sphalerite structure within the ordered sphalerite phase. This modification caused the energy band at the interface to bend, thereby generating energy barriers that effectively scatter low-energy carriers. As a result, both the *S* and σ were improved. Jolly Jacob et al[58] adopted a similar strategy by doping Cd into Cu_2ZnSnS_4 and found that the *S* increased with adding Cd. They found that, Cd doping led to the formation of Cu-based secondary phases. These secondary phases serve as effective filters for low-energy carriers, while allowing only high-energy carriers to pass through, thereby improving the performance of material. Additionally, introducing spin entropy by doping magnetic particles such as Ni[59] or elements such as Pb and Te[60] can effectively increase the effective mass and improve the *S* of the material.

3 Optimization of Thermal Transport Performance

We know that the transfer of thermal energy is mainly achieved through lattice vibrations and carrier transport, with the former represented as lattice thermal conductivity κ_l and the latter as electronic thermal conductivity κ_e. They can be

represented as:

$$\kappa_l = \frac{1}{3} C_V \upsilon l \quad (5)$$

$$\kappa_e = L\sigma T \quad (6)$$

In the above equation, C_v is specific heat at constant volume of materials, υ is phonon velocity, l is mean free path of phonon collision[61], L is Lorentz constant. Although the complex crystal structure and elemental composition of Cu-based quaternary diamondoid materials result in relatively low intrinsic thermal conductivity, there is still room for further optimization. Unlike κ_e, κ_l is almost independent of other electronic transport parameters, and can be regulated independently. To this end, many researchers have focused on reducing the κ_l to improve the thermoelectric performance. Defect control and microstructure design are two effective methods for reducing κ_l.

3.1 Defect Control

Compared to C_v and υ, the l is easier to regulate, particularly through controlling the defects state in the material. So far, introducing appropriate defects into the lattice to reduce the l has remained the main strategy for suppressing κ_l. The impact of point defects mainly lies in the fluctuation of the mass field caused by different atomic masses and the fluctuation of the stress field caused by different atomic radii. The larger the difference, the stronger the scattering effect on high-frequency phonons, and the better the result in reducing κ_l. For example, Qiufan Chen et al[57] prepared Ag-doped $Cu_2CdSnSe_4$ using a chemical method, which introduced Ag_{Cu} point defects into the

matrix, distorting the crystal structure and enhancing the phonon scattering. In addition, Qingfeng Song et al[62] introduced excess Cu into $Cu_2MnSnSe_4$, increasing local lattice distortion and suppressing κ_l. Studies also indicate that replacing Zn with Co in $Cu_2ZnSnSe_4$ increases point defects, reduces phonon relaxation time, and thus decrease κ_l [63]. Besides, anionic substitution significantly reduces the κ_l of $Cu_2ZnGeSe_{4-x}S_x$[64], primarily due to the disorder caused by substitution. Ultra-low κ_l can also be achieved in the locally disordered $Cu_{2+x}Zn_{1-x}SnS_4$[43], which is mainly attributed to the highly disordered arrangement of Cu and Zn in the lattice, causing phonon localization and shortening the phonon mean free path. Some researchers also use lattice strain to regulate the thermoelectric properties of materials[65]. They introduce lattice strain by creating dislocations, which reduce the relaxation time of phonons and enhance their scattering, as shown in **Figure 7**.

3.2 Microstructure Design

In addition to introducing point defects, microstructure design, such as nano precipitate, nanocrystalline material, and secondary phase boundary, can also reduce κ_l. For example, Feng-Jia Fan et al[66] synthesized $Cu_2CdSnSe_4$ nanocrystals through colloidal synthesis and prepared bulk materials by hot pressing. In their work, the nanocrystals generated more grain boundaries, significantly enhancing phonon scattering. This ultimately resulted in a thermal conductivity of 1.7 W m^{-1} K^{-1}at room temperature, which is about 40% lower than that of the bulk sample prepared by solid-state reaction. After that, Kaya Wei et al[67] reported the preparation of nanostructured

$Cu_2ZnSnSe_4$ and $Ag_2ZnSnSe_4$, once again confirming the impact of nanomaterials on the κ_l of these materials. Combining bulk materials with nanocrystals can reduce thermal conductivity while maintaining the high electrical properties of the bulk material. Qiufan Chen et al[68] prepared $Cu_2CdSnSe_4$ nanocrystals using colloidal synthesis and added these nanocrystals into the $Cu_2CdSnSe_4$ matrix, as shown in **Figure 8**. They found that this hierarchical architecture is able to suppress the thermal conductivity while preserving the decent electrical properties. The increased grain boundaries and embedded nanocrystals significantly enhanced phonon scattering, especially the latter serving as additional scattering centers that effectively scatter medium to long wavelength phonons, thereby reducing κ_l. Himanshu Nautiyal et al[69] synthesized disordered nanostructured polycrystals of Cu_2ZnSnS_4 and $Cu_2ZnSnSe_4$ through high-energy reaction mechanical alloying, achieving a low thermal conductivity of 0.2 W m^{-1} K^{-1}. Similar studies have also been conducted by Binayak Mukherjee et al[70], who obtained cubic $Cu_2ZnSnSe_4$ nanostructures with a low thermal conductivity of 0.21W m^{-1} K^{-1}.

The optimization of thermal conductivity through grain boundary engineering through the introduction of a secondary phase has also been proven to be an effective method. The interface between the secondary phase and the matrix generates strong phonon scattering. Yingcai Zhu et al[71] replaced Sn with Pb in $Cu_2ZnSnSe_4$ and found that Pb primarily exists in the PbSe framework, distributed as a secondary phase at grain boundaries, as shown in **Figure 9**. The phase interface between the secondary phase and the matrix has a strong scattering effect on phonons. Additionally, the smaller grain

size of the secondary phase increases the density of grain boundaries and further reduces the κ_l. Furthermore, the composite of CdSe and $Cu_2CdSnSe_4$ forms a coherent phase interface, allowing charge carriers to pass through while scattering phonons across a wide frequency spectrum[72]. The Cd vaporization during the hot pressing, creating nanopores in the material that introduce additional scattering centers, significantly reducing the κ_l.

4 Summary and Outlook

Recently, diamondoid thermoelectric materials have gained significant attention due to their unique electronic and thermal transport properties. Although their thermoelectric performance has yet to reach the levels of traditional thermoelectric materials, they are still a new star with great research potential. This article focuses on Cu-based quaternary diamondoid materials and provides a collection of recent progress and a comprehensive view of the optimization strategies for improving their electrical and thermal properties. We have thoroughly discussed the influence of various defects on the carrier concentration, carrier mobility and the band structure of the Cu-based quaternary diamondoid materials. Additionally, we have summarized a series of effective methods to enhance the phonon scattering and suppress the thermal conductivity. Overall, improving the carrier mobility while further reducing the thermal conductivity is critical for achieving high thermoelectric performance in these materials. In this context, the recently proposed off-centering effect may offer a new perspective and provide promising pathways for future optimization. In summary, although

significant progress has been made in promoting the thermoelectric performance of these systems, many challenges remain unresolved. We hope this review provide fresh insights and sparks new ideas for further improving the thermoelectric performance of these promising materials.

Competing interests

The authors declare no competing interests.

Acknowledgements

This work was primarily supported by the National Natural Science Foundation of China (52471217), National Science Fund for Distinguished Young Scholars (51925101), National Natural Science Foundation of China (52450001, 52250090, 52371208, 52002042, 51772012, 51571007, and 12374023), the Beijing Natural Science Foundation (JO18004), and the 111 Project (B17002). L. D. Z. appreciates the support from the Tencent Xplorer Prize.

References

[1] Xie, H.,Zhao, L. D.,Kanatzidis, M. G., *Interdiscip. Mater.*, 2024, 3, 51.

[2] Liu, Y.,Xie, H.,Li, Z.,Zhang, Y.,Malliakas, C. D.,Al Malki, M.,Ribet, S.,Hao, S.,Pham, T.,Wang, Y.,Hu, X.,dos Reis, R.,Snyder, G. J.,Uher, C.,Wolverton, C.,Kanatzidis, M. G.,Dravid, V. P., *J. Am. Chem. Soc.*, 2023, 145, 8677.

[3] Xie, H. Y.,Su, X. L.,Hao, S. Q.,Wolverton, C.,Uher, C.,Tang, X. F.,Kanatzidis, M. G., *Phys. Rev. Mater.*, 2020, 4, 2.

[4] Zheng, Z.,Su, X. L.,Deng, R. G.,Stoumpos, C.,Xie, H. Y.,Liu, W.,Yan, Y. G.,Hao, S. Q.,Uher, C.,Wolverton, C.,Kanatzidis, M. G.,Tang, X. F., *J. Am. Chem. Soc.*, 2018, 140, 7.

[5] Xie, H. Y.,Zhao, L. D., *Mater. Futures*, 2024, 3, 1.

[6] Xie, H. Y.,Su, X. L.,Bailey, T. P.,Zhang, C.,Liu, W.,Uher, C.,Tang, X. F.,Kanatzidis, M. G., *Chem. Mater.*, 2020, 32, 6.

[7] Liu, D. R.,Wang, D. Y.,Hong, T.,Wang, Z. Y.,Wang, Y. P.,Qin, Y. X.,Su, L. Z.,Yang, T. Y.,Gao, X.,Ge, Z. H.,Qin, B. C.,Zhao, L. D., *Science*, 2023, 380, 6647.

[8] Zheng, Y.,Zhang, Q.,Su, X. L.,Xie, H. Y.,Shu, S. C.,Chen, T. L.,Tan, G. J.,Yan, Y. G.,Tang, X. F.,Uher, C.,Snyder, G. J., *Adv. Energy Mater.*, 2015, 5, 5.

[9] Gao, D. Z.,Wang, S. N.,Wen, Y.,Fang, F.,Li, Y. C.,Liu, S. B.,Wang, Y. K.,Xie, H. Y.,Qiu, Y. T.,Zhao, L. D., *Mater. Today Phys.*, 2024, 41.

[10] Xie, H.,Hao, S.,Bao, J.,Slade, T. J.,Snyder, G. J.,Wolverton, C.,Kanatzidis, M. G., *J. Am. Chem. Soc.*, 2020, 142, 955320.

[11] Zheng, G.,Su, X. L.,Xie, H. Y.,Shu, Y. J.,Liang, T.,She, X. Y.,Liu, W.,Yan, Y. G.,Zhang, Q. J.,Uher, C.,Kanatzidis, M. G.,Tang, X. F., *Energy Environ. Sci.*, 2017, 10, 12.

[12] He, J.,Tritt, T. M., *Science*, 2017, 357, 6358.

[13] Bai, S. L.,Zhang, X.,Zhao, L. D., *Acc. Chem. Res.*, 2023, 56, 21.

[14] Zhao, L. D.,Lo, S. H.,Zhang, Y. S.,Sun, H.,Tan, G. J.,Uher, C.,Wolverton, C.,Dravid, V. P.,Kanatzidis, M. G., *Nature*, 2014, 508, 7496.

[15] Zhao, L. D.,Tan, G. J.,Hao, S. Q.,He, J. Q.,Pei, Y. L.,Chi, H.,Wang, H.,Gong, S. K.,Xu, H. B.,Dravid, V. P.,Uher, C.,Snyder, G. J.,Wolverton, C.,Kanatzidis, M. G., *Science*, 2016, 351, 6269.

[16] Bozin, E. S.,Xie, H.,Abeykoon, A. M. M.,Everett, S. M.,Tucker, M. G.,Kanatzidis, M. G.,Billinge, S. J. L., *Phys. Rev. Lett.*, 2023, 131, 3.

[17] Qiu, J. H.,Yan, Y. G.,Luo, T. T.,Tang, K. C.,Yao, L.,Zhang, J.,Zhang, M.,Su, X. L.,Tan, G. J.,Xie, H. Y.,Kanatzidis, M. G.,Uher, C.,Tang, X. F., *Energy Environ. Sci.*, 2019, 12, 10.

[18] Zhu, B.,Liu, X. X.,Wang, Q.,Qiu, Y.,Shu, Z.,Guo, Z. T.,Tong, Y.,Cui, J.,Gu, M.,He, J. Q., *Energy Environ. Sci.*, 2020, 13, 7.

[19] Wang, L.,Wen, Y.,Bai, S. L.,Chang, C.,Li, Y. C.,Liu, S.,Liu, D. R.,Wang, S. Q.,Zhao, Z.,Zhan, S. P.,Cao, Q.,Gao, X.,Xie, H. Y.,Zhao, L. D., *Nat. Commun.*, 2024, 15, 1.

[20] Wang, S. Q.,Wen, Y.,Zhu, Y. C.,Wang, Z. Y.,Liu, D. R.,Zheng, J. Q.,Zhan, S. P.,Xie, H. Y.,Ge, Z. H.,Gao, X.,Cao, Q.,Chang, C.,Zhao, L. D., *Small*, 2024, 20, 202400866.

[21] Pang, H. M.,Qin, Y. X.,Qin, B. C.,Yu, L. X.,Su, X. L.,Liang, H.,Ge, Z. H.,Cao, Q.,Tan, Q.,Zhao, L. D., *Adv. Funct. Mater.*, 2024, 34, 202401716.

[22] Liu, S. B.,Wen, Y.,Bai, S. L.,Shi, H. A.,Qin, Y. X.,Qin, B. C.,Liu, D. R.,Cao, Q.,Gao, X.,Su, L. Z.,Chang, C.,Zhang, X.,Zhao, L. D., *Adv. Mater.*, 2024, 36, 25.

[23] Chen, X. X.,Wu, H. J.,Cui, J.,Xiao, Y.,Zhang, Y.,He, J. Q.,Chen, Y.,Cao, J.,Cai,

W.,Pennycook, S. J.,Liu, Z. H.,Zhao, L. D.,Sui, J. H., *Nano Energy*, 2018, 52, 246.

[24] Li, D.,Zhang, B. L.,Ming, H. W.,Wang, L.,Zu, Y.,Qin, X. Y., *ACS Appl. Mater. Interfaces*, 2021, 13, 29.

[25] Vinodhini, J.,Shalini, V.,Harish, S.,Ikeda, H.,Archana, J.,Navaneethan, M., *J. Colloid Interface Sci.*, 2023, 651, 436.

[26] Imasato, K.,Kang, S. D.,Ohno, S.,Snyder, G. J., *Mater. Horiz.*, 2018, 5, 1.

[27] Xie, H.,Liu, Y.,Zhang, Y.,Hao, S.,Li, Z.,Cheng, M.,Cai, S.,Snyder, G. J.,Wolverton, C.,Uher, C.,Dravid, V. P.,Kanatzidis, M. G., *J. Am. Chem. Soc.*, 2022, 144, 911320.

[28] Yu, J. J.,Fu, C. G.,Liu, Y. T.,Xia, K. Y.,Aydemir, U.,Chasapis, T. C.,Snyder, G. J.,Zhao, X. B.,Zhu, T. J., *Adv. Energy Mater.*, 2018, 8, 1.

[29] Cheng, X.,Zhu, B.,Yang, D.,Su, X.,Liu, W.,Xie, H.,Zheng, Y.,Tang, X., *ACS Appl. Mater. Interfaces*, 2022, 14, 54394.

[30] Hu, L.,Luo, Y. B.,Fang, Y. W.,Qin, F. Y.,Cao, X.,Xie, H. Y.,Liu, J. W.,Dong, J. F.,Sanson, A.,Giarola, M.,Tan, X. Y.,Zheng, Y.,Suwardi, A.,Huang, Y. Z.,Hippalgaonkar, K.,He, J. Q.,Zhang, W. Q.,Xu, J. W.,Yan, Q. Y.,Kanatzidis, M. G., *Adv. Energy Mater.*, 2021, 11, 42.

[31] Cheng, X.,Yang, D.,Su, X.,Xie, H.,Liu, W.,Zheng, Y.,Tang, X., *ACS Appl. Mater. Interfaces*, 2021, 13, 5517846.

[32] Cao, Y.,Su, X.,Meng, F.,Bailey, T. P.,Zhao, J.,Xie, H.,He, J.,Uher, C.,Tang, X., *Adv. Funct. Mater.*, 2020, 30, 51.

[33] Shi, X. Y.,Huang, F. Q.,Liu, M. L.,Chen, L. D., *Appl. Phys. Lett.*, 2009, 94, 12.

[34] Liu, M. L.,Chen, I. W.,Huang, F. Q.,Chen, L. D., *Adv. Mater.*, 2009, 21, 380837.

[35] Xie, H.,Hao, S.,Cai, S.,Bailey, T. P.,Uher, C.,Wolverton, C.,Dravid, V. P.,Kanatzidis, M. G.,

Energy Environ. Sci., 2020, 13, 369310.

[36] Liu, R. H.,Xi, L. L.,Liu, H. L.,Shi, X.,Zhang, W. Q.,Chen, L. D., *Chem. Commun.*, 2012, 48, 32.

[37] Plirdpring, T.,Kurosaki, K.,Kosuga, A.,Day, T.,Firdosy, S.,Ravi, V.,Snyder, G. J.,Harnwunggmoung, A.,Sugahara, T.,Ohishi, Y.,Muta, H.,Yamanaka, S., *Adv. Mater.*, 2012, 24, 27.

[38] Xie, H.,Li, Z.,Liu, Y.,Zhang, Y.,Uher, C.,Dravid, V. P.,Wolverton, C.,Kanatzidis, M. G., *J. Am. Chem. Soc.*, 2023, 145, 32115.

[39] Xie, H. Y.,Bozin, E. S.,Li, Z.,Abeykoon, M.,Banerjee, S.,Male, J. P.,Snyder, G. J.,Wolverton, C.,Billinge, S. J. L.,Kanatzidis, M. G., *Adv. Mater.*, 2022, 34, 24.

[40] Xie, H. Y.,Su, X. L.,Zheng, G.,Zhu, T.,Yin, K.,Yan, Y. G.,Uher, C.,Kanatzidis, M. G.,Tang, X. F., *Adv. Energy Mater.*, 2017, 7, 3.

[41] Xie, H. Y.,Su, X. L.,Hao, S. Q.,Zhang, C.,Zhang, Z. K.,Liu, W.,Yan, Y. G.,Wolverton, C.,Tang, X. F.,Kanatzidis, M. G., *J. Am. Chem. Soc.*, 2019, 141, 47.

[42] Liu, M.-L.,Huang, F.-Q.,Chen, L.-D.,Chen, I. W., *Appl. Phys. Lett.*, 2009, 94, 20.

[43] Jiang, Q.,Yan, H.,Lin, Y.,Shen, Y.,Yang, J.,Reece, M. J., *J. Mater. Chem. A*, 2020, 8, 1090921.

[44] Dong, Y.,Wang, H.,Nolas, G. S., *PHYS STATUS SOLIDI-R*, 2013, 8, 611.

[45] Li, Z.,Zhang, W.,Gu, B.,Zhao, C.,Ye, B.,Xiao, C.,Xie, Y., *J. Mater. Chem. A*, 2021, 9, 10062.

[46] Liu, F. S.,Zheng, J. X.,Huang, M. J.,He, L. P.,Ao, W. Q.,Pan, F.,Li, J. Q., *Sci. Rep.*, 2014, 4, 1.

[47] Wang, B.,Li, Y.,Zheng, J. X.,Xu, M.,Liu, F. S.,Ao, W. Q.,Li, J. Q.,Pan, F., *Sci. Rep.*, 2015,

5, 9365.

[48] Chetty, R.,Bali, A.,Mallik, R. C., *Intermetallics*, 2016, 72, 17.

[49] Mehmood, F.,Sun, Y.,Su, W.,Chebanova, G.,Zhai, J.,Wang, L.,Khan, M.,Romanenko, A.,Wang, H.,Wang, C., *PHYS STATUS SOLIDI-R*, 2022, 16, 6.

[50] Wei, K.,Beauchemin, L.,Wang, H.,Porter, W. D.,Martin, J.,Nolas, G. S., *J. Alloys Compd.*, 2015, 650, 844.

[51] Song, Q.,Qiu, P.,Chen, H.,Zhao, K.,Guan, M.,Zhou, Y.,Wei, T. R.,Ren, D.,Xi, L.,Yang, J.,Chen, Z.,Shi, X.,Chen, L., *Mater. Today Phys.*, 2018, 7, 45.

[52] Parashchuk, T.,Cherniushok, O.,Smitiukh, O.,Marchuk, O.,Wojciechowski, K. T., *Chem. Mater.*, 2023, 35, 477212.

[53] Sharma, S. D.,Bayikadi, K.,Raman, S.,Neeleshwar, S., *Nanotechnology*, 2020, 31, 36540236.

[54] Ashfaq, A.,Ali, A.,Mahmood, K.,Rehman, U. u.,Tahir, S.,Amin, N.,Ahmad, W.,Aslam, R. N.,Arshad, M.,Rasheed, K., *Ceram. Int.*, 2021, 47, 3535624.

[55] Isotta, E.,Fanciulli, C.,Pugno, N. M.,Scardi, P., *Nanomaterials*, 2019, 9, 7625.

[56] Nagaoka, A.,Yoshino, K.,Masuda, T.,Sparks, T. D.,Scarpulla, M. A.,Nishioka, K., *J. Mater. Chem. A*, 2021, 9, 1559528.

[57] Chen, Q. F.,Wang, G. W.,Zhang, A. J.,Yang, D. F.,Yao, W.,Peng, K. L.,Yan, Y. C.,Sun, X. N.,Liu, A. P.,Wang, G. Y.,Zhou, X. Y., *J. Mater. Chem. C*, 2015, 3, 47.

[58] Jacob, J.,Ali, H. T.,Ali, A.,Mehboob, K.,Ashfaq, A.,Ikram, S.,Rehman, U.,Mahmood, K.,Amin, N., *Mater. Sci. Semicond. Process.*, 2021, 123, 105587.

[59] Xiao, C.,Li, K.,Zhang, J. J.,Tong, W.,Liu, Y. W.,Li, Z.,Huang, P. C.,Pan, B. C.,Su, H. B.,Xie,

Y., *Mater. Horiz.*, 2014, 1, 1.

[60] Huo, T.,Mehmood, F.,Wang, H.,Su, W.,Wang, X.,Chen, T.,Zhang, K.,Feng, J.,Wang, C., *Phys. Status Solidi A*, 2020, 217, 17.

[61] Xie, H. Y.,Su, X. L.,Zhang, X. M.,Hao, S. Q.,Bailey, T. P.,Stoumpos, C. C.,Douvalis, A. P.,Hu, X. B.,Wolverton, C.,Dravid, V. P.,Uher, C.,Tang, X. F.,Kanatzidis, M. G., *J. Am. Chem. Soc.*, 2019, 141, 27.

[62] Song, Q.,Qiu, P.,Chen, H.,Zhao, K.,Ren, D.,Shi, X.,Chen, L., *ACS Appl. Mater. Interfaces*, 2018, 10, 1012312.

[63] Zhu, Y.,Liu, Y.,Ren, G.,Tan, X.,Yu, M.,Lin, Y.-H.,Nan, C.-W.,Marcelli, A.,Hu, T.,Xu, W., *Inorg. Chem.*, 2018, 57, 605110.

[64] Heinrich, C. P.,Day, T. W.,Zeier, W. G.,Snyder, G. J.,Tremel, W., *J. Am. Chem. Soc.*, 2013, 136, 4421.

[65] Sun, Y.,Abbas, A.,Wang, H.,Tan, C.,Li, Z.,Zong, Y.,Sun, H.,Wang, C.,Wang, H., *Chem. Eng. J.*, 2024, 486, 150158.

[66] Fan, F.-J.,Yu, B.,Wang, Y.-X.,Zhu, Y.-L.,Liu, X.-J.,Yu, S.-H.,Ren, Z., *J. Am. Chem. Soc.*, 2011, 133, 1591040.

[67] Wei, K.,Nolas, G. S., *ACS Appl. Mater. Interfaces*, 2015, 7, 975218.

[68] Chen, Q.,Yan, Y.,Zhan, H.,Yao, W.,Chen, Y.,Dai, J.,Sun, X.,Zhou, X., *J. Materiomics*, 2016, 2, 1792.

[69] Nautiyal, H.,Lohani, K.,Mukherjee, B.,Isotta, E.,Malagutti, M. A.,Ataollahi, N.,Pallecchi, I.,Putti, M.,Misture, S. T.,Rebuffi, L.,Scardi, P., *Nanomaterials*, 2023, 13, 3662.

[70] Mukherjee, B.,Isotta, E.,Malagutti, M. A.,Lohani, K.,Rebuffi, L.,Fanciulli, C.,Scardi, P., *J.*

Alloys Compd., 2023, 933, 167756.

[71] Zhu, Y.,Liu, Y.,Tan, X.,Ren, G.,Yu, M.,Hu, T.,Marcelli, A.,Xu, W., *AIP Adv.*, 2018, 8, 4.

[72] Basu, R.,Mandava, S.,Bohra, A.,Bhattacharya, S.,Bhatt, R.,Ahmad, S.,Bhattacharyya, K.,Samanta, S.,Debnath, A. K.,Singh, A.,Aswal, D. K.,Muthe, K. P.,Gadkari, S. C., *J. Electron. Mater.*, 2019, 48, 4.

[73] El Hamdaoui, J. E.,Kria, M.,Lakaal, K.,El-Yadri, M.,Feddi, E. M.,Pedraja Rejas, L. P.,Pérez, L. M.,Díaz, P.,Mora-Ramos, M. E.,Laroze, D., *Int. J. Mol. Sci.*, 2022, 23, 1278521.

[74] Zeier, W. G.,LaLonde, A.,Gibbs, Z. M.,Heinrich, C. P.,Panthöfer, M.,Snyder, G. J.,Tremel, W., *J. Am. Chem. Soc.*, 2012, 134, 16.

[75] Kumar, V. P.,Guilmeau, E.,Raveau, B.,Caignaert, V.,Varadaraju, U. V., *Journal of Applied Physics*, 2015, 118, 15.

[76] Chetty, R.,Dadda, J.,de Boor, J.,Müller, E.,Mallik, R. C., *Intermetallics*, 2015, 57, 156.

[77] Ibáñez, M.,Zamani, R.,LaLonde, A.,Cadavid, D.,Li, W. H.,Shavel, A.,Arbiol, J.,Morante, J. R.,Gorsse, S.,Snyder, G. J.,Cabot, A., *Journal of the American Chemical Society*, 2012, 134, 9.

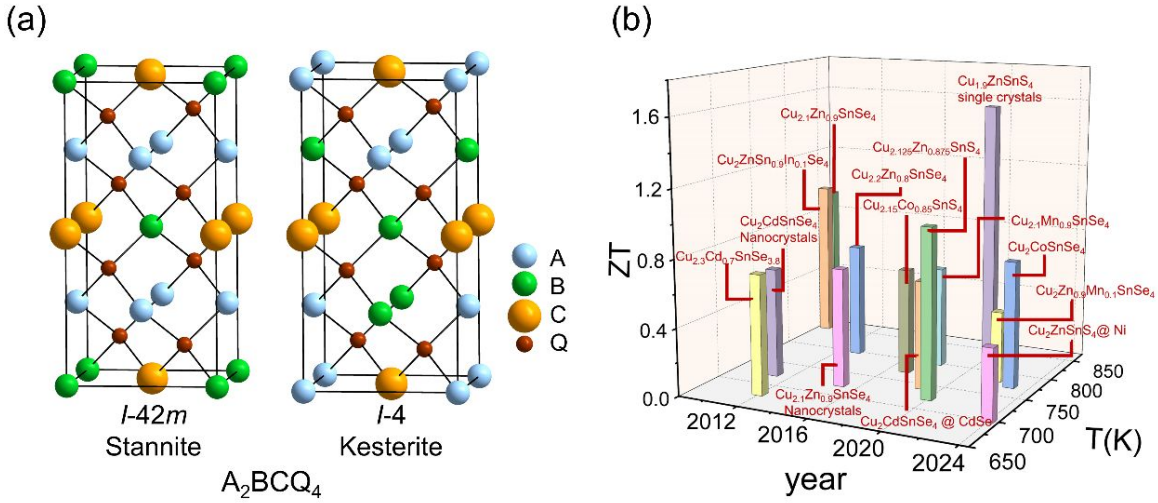

Figure 1 The development of quaternary diamondoid thermoelectric materials. (a) Structure of quaternary diamondoid thermoelectric materials. (b) Current state of the art quaternary diamondoid thermoelectric materials, the figure - of - merit *ZT* as a function of temperature and the published time.

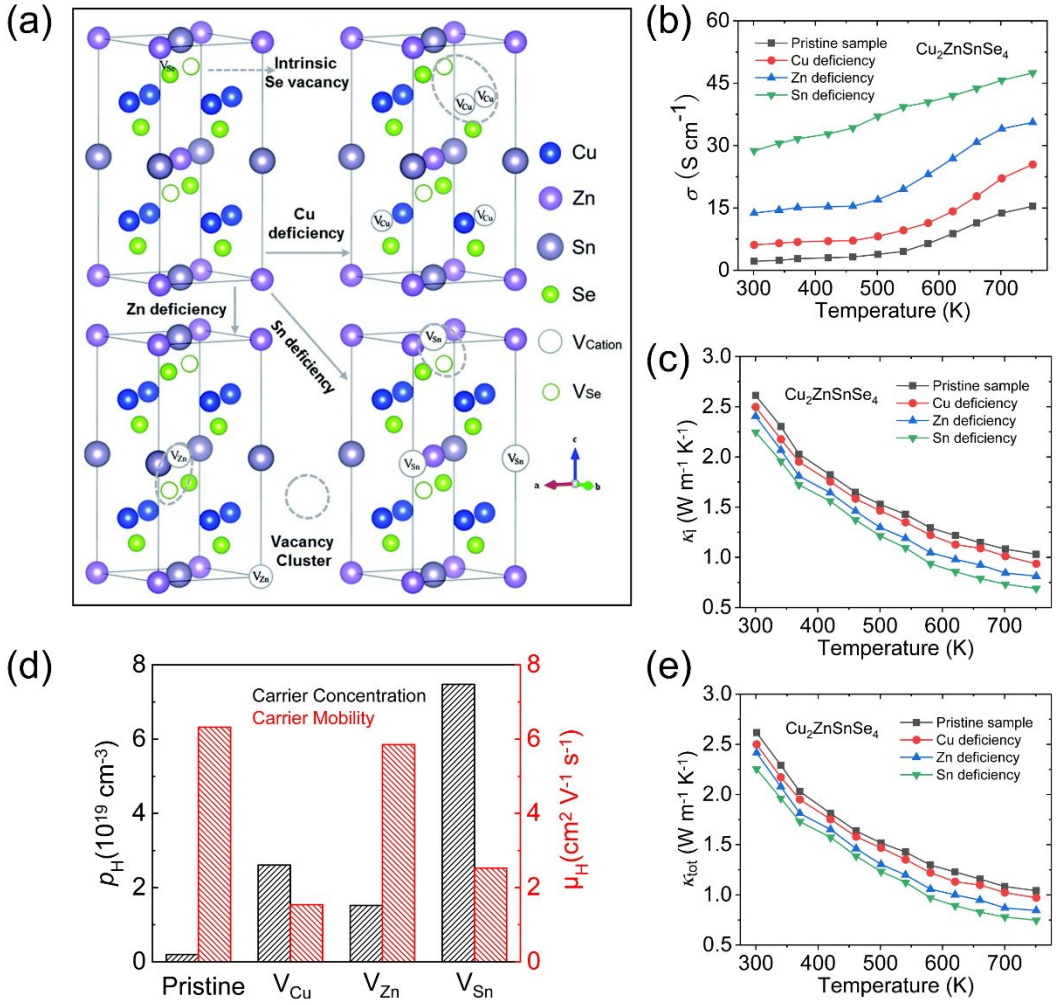

Figure 2 The influence of different cation vacancies on thermoelectric transport properties for $Cu_2ZnSnSe_4$. (a) Schematic diagram of different cation vacancies in $Cu_2ZnSnSe_4$. Temperature dependence of (b) Electric conductivity (σ) and (c) Lattice thermal conductivity (κ_l). (d) The room temperature of carrier concentration (p_H) and mobility(μ_H) for different samples. (e) Total thermal conductivity (κ_{tot}) as a function of temperature.

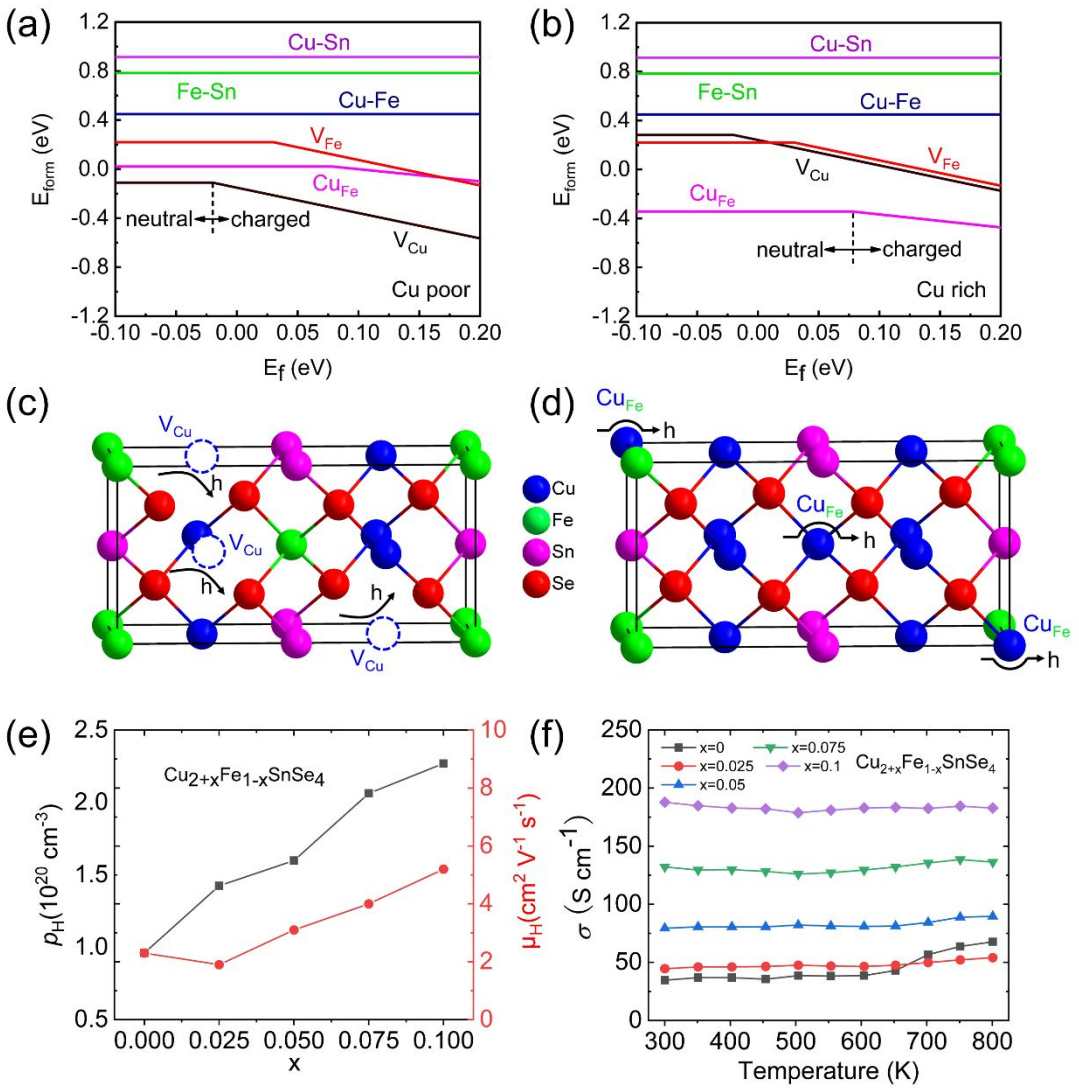

Figure 3 The influence of different defects on carrier transport in $Cu_2FeSnSe_4$. (a) Defect formation energy of Cu-poor conditions. (b) Defect formation energy of Cu-rich conditions. Schematic diagram of charge carriers scattering by (c) V_{Cu} vacancy and (d) Cu_{Fe} anti-site defect. (e) The room temperature carrier concentration (p_H) and mobility (μ_H) for $Cu_{2+x}Fe_{1-x}SnSe_4$. (f) Electric conductivity (σ) as a function of temperature for $Cu_{2+x}Fe_{1-x}SnSe_4$.

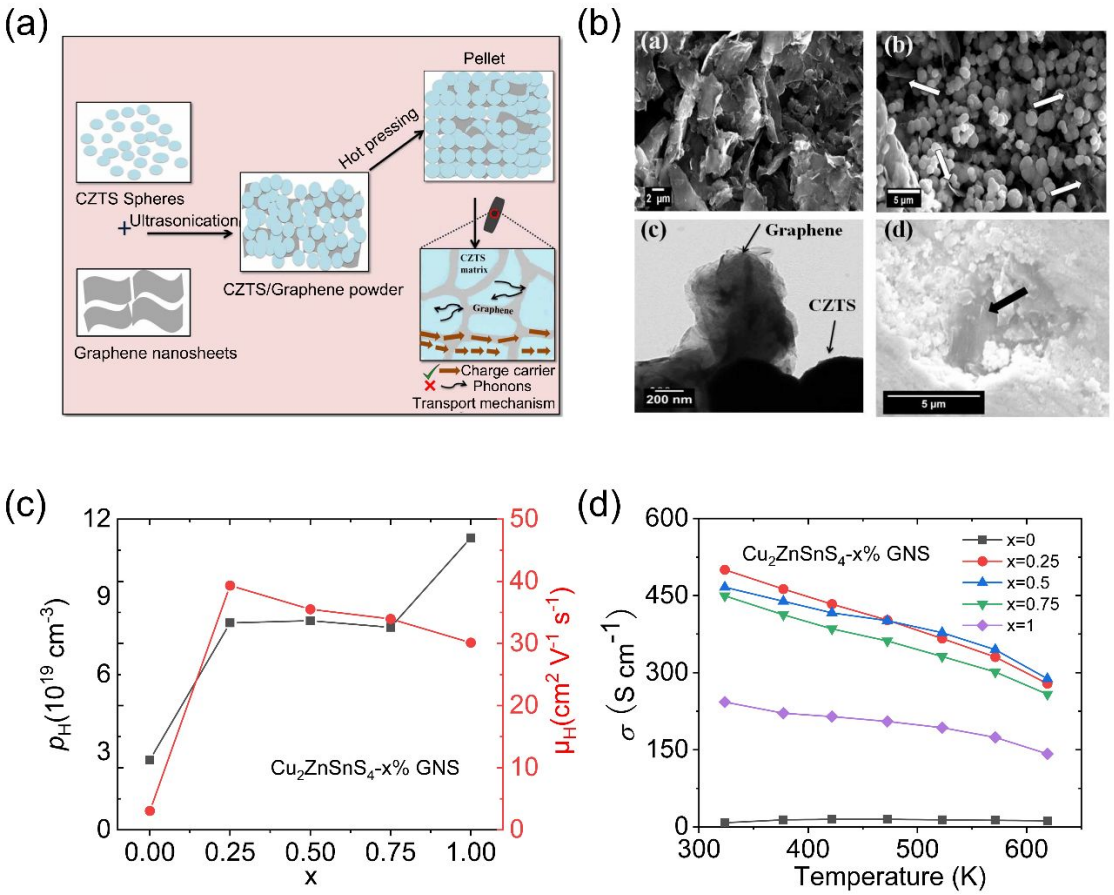

Figure 4 Introducing graphene to improve the electrical transport performance of Cu_2ZnSnS_4. (a) Schematic diagram shows the microstructure of sample. (b) SEM micrographs and TEM image of Cu_2ZnSnS_4/0.75 wt% GNs composite powder. (c) The room temperature carrier concentration (p_H) and mobility (μ_H) of graphene doped samples. (d) Temperature dependence of electric conductivity (σ).

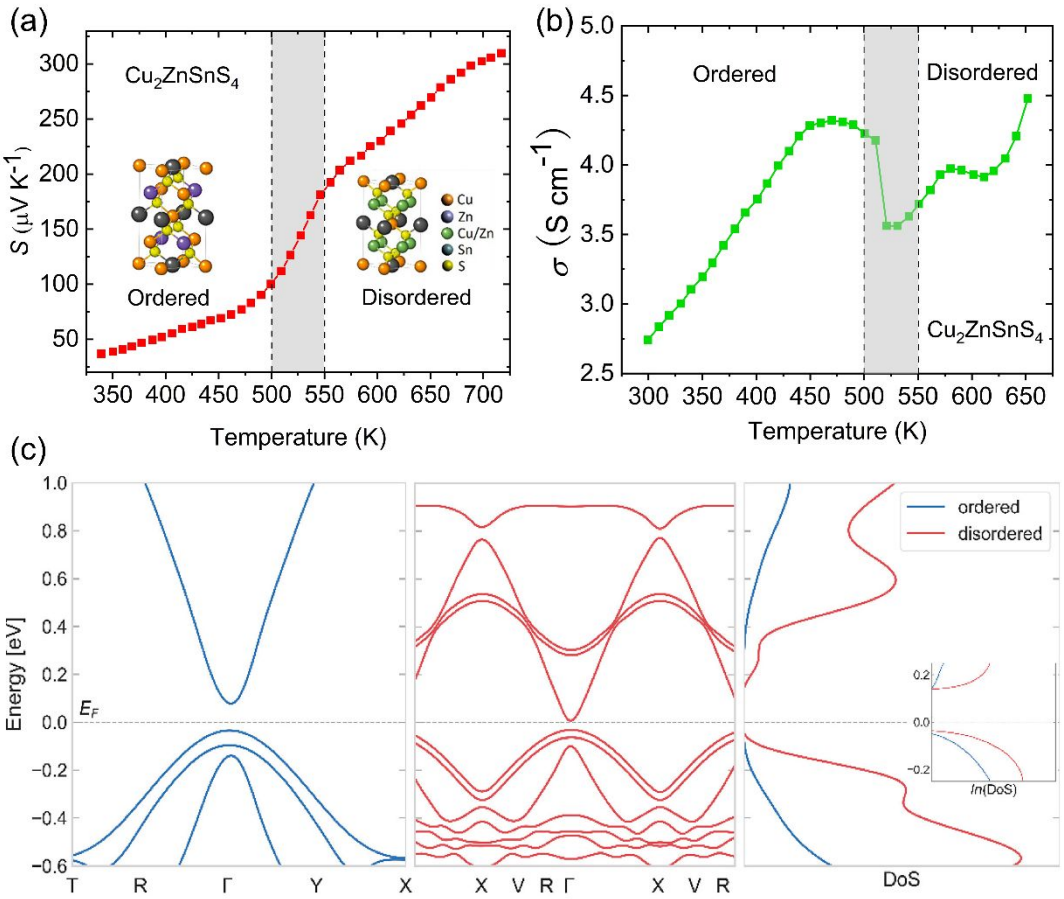

Figure 5 The influence of ordered and disordered structure on electrical transport performance of Cu_2ZnSnS_4. Temperature dependence of (a) Seebeck coefficient (S) and (b) electric conductivity (σ). (c) The band structures and density of states for ordered and disordered Cu_2ZnSnS_4.

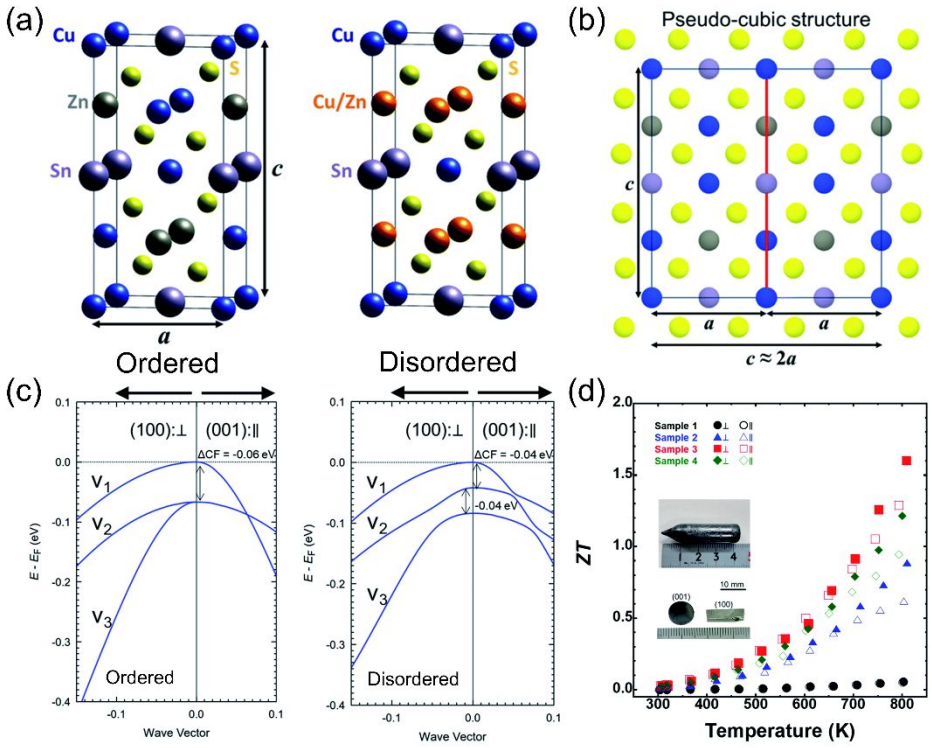

Figure 6 The crystal structure and transport properties of Cu_2ZnSnS_4. (a) The crystal structures of ordered and disordered Cu_2ZnSnS_4. (b) Pseudo-cubic structure shows the crystal structure parameter η (c/2a) ≈ 1. (c) The valence bands for the ordered and disordered Cu_2ZnSnS_4. (d) Temperature dependence of *ZT* for Cu_2ZnSnS_4 single crystals with different composition.

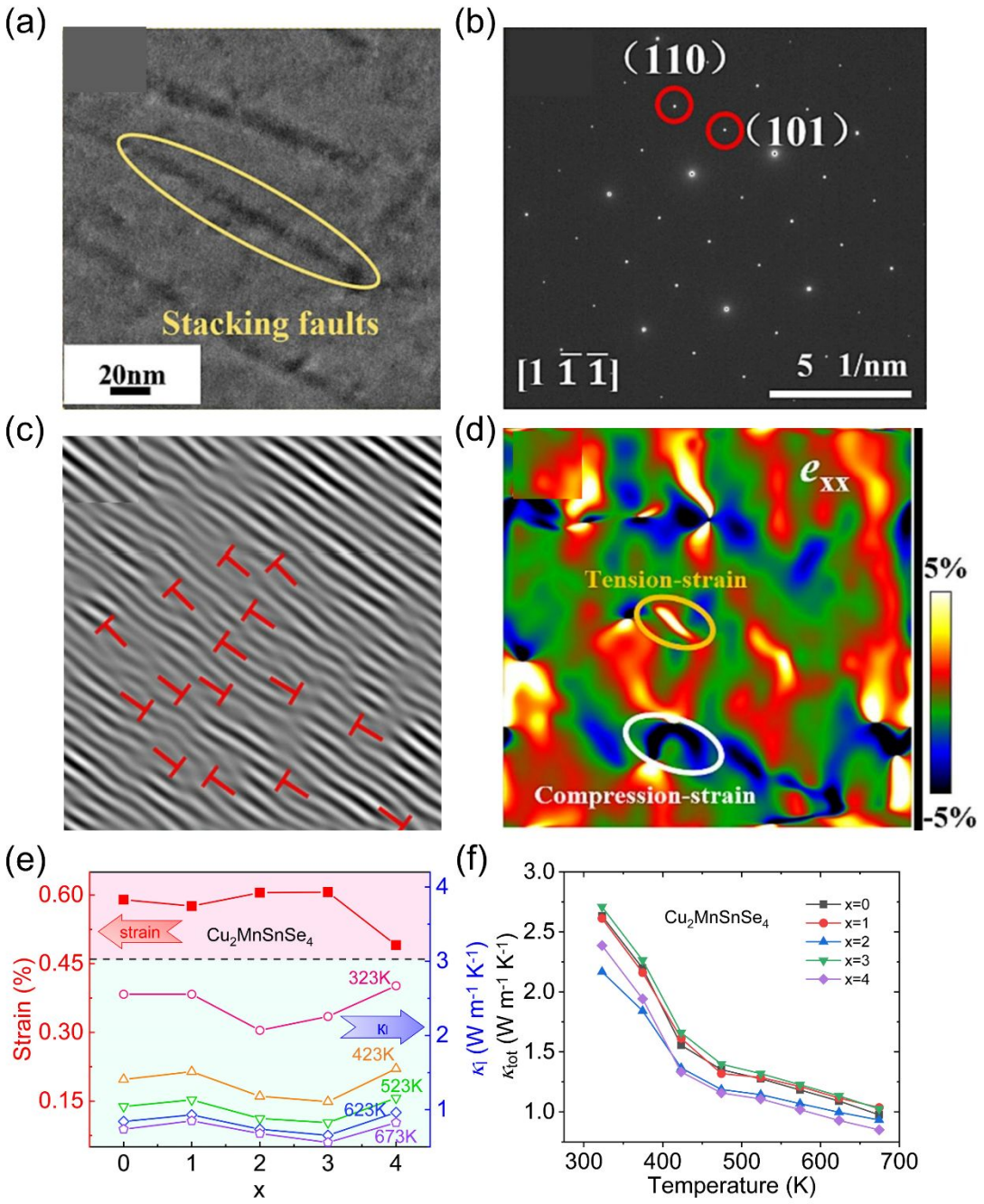

Figure 7 The influence of lattice strain on thermal conductivity. (a) The TEM image of $Cu_2MnSnSe_4$ showing the stacking faults in the matrix. (b) SAED pattern of $Cu_2MnSnSe_4$ along [1 -1 -1] direction. (c) The IFFT image showing dislocation in the material. (d) The corresponding strain mapping of $Cu_2MnSnSe_4$ lattice. (e) The lattice thermal conductivity (κ_l) and lattice strain of $Cu_2MnSnSe_4$. (f) Temperature dependence of total thermal conductivity (κ_{tot}) of $Cu_2MnSnSe_4$.

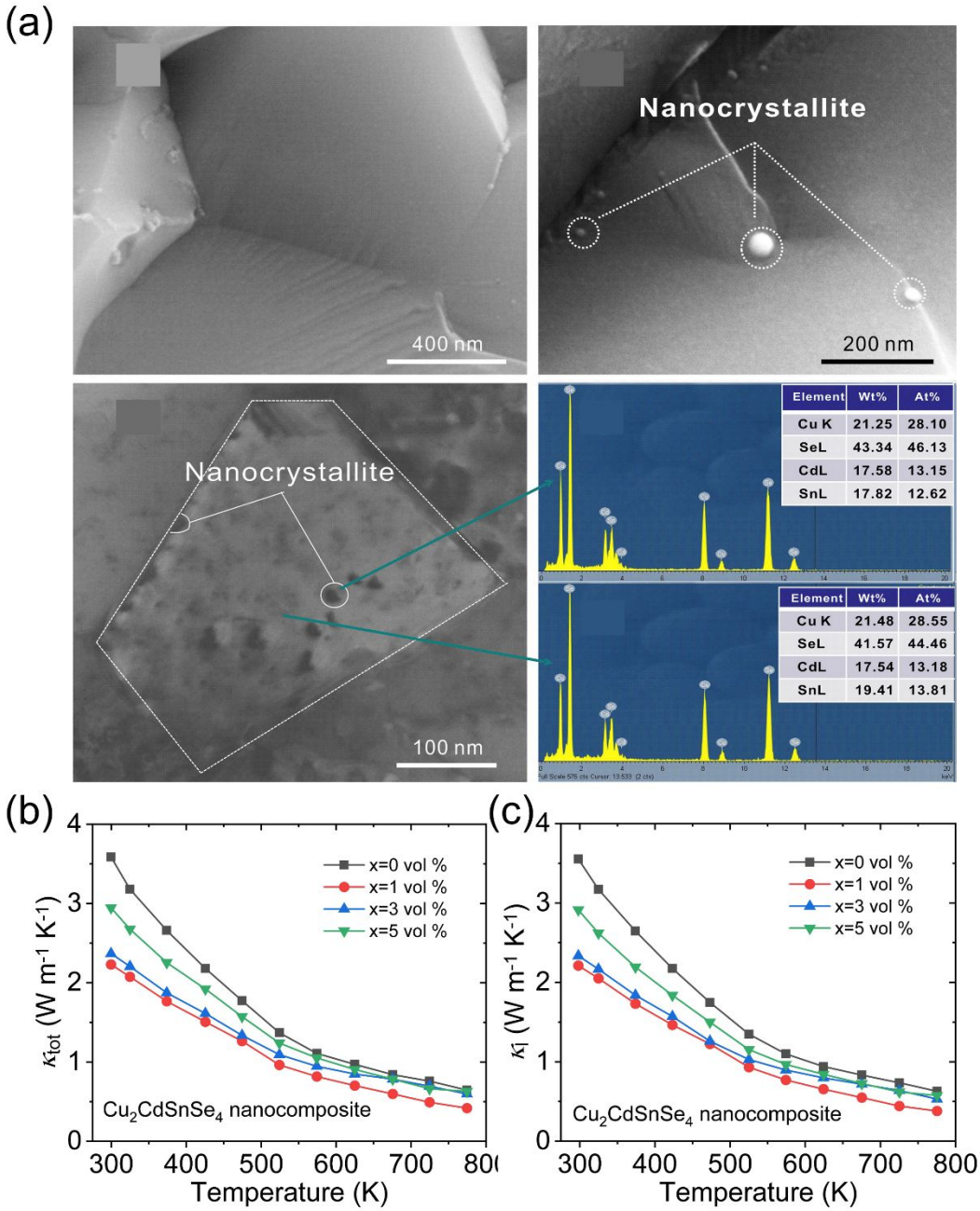

Figure 8 Morphology and thermal properties of nanocomposite materials. (a) The morphology of fracture surface for $Cu_2CdSnSe_4$ matrix and the nanocomposite. Temperature dependence of (b) total thermal conductivity (κ_{tot}) and (c) lattice thermal conductivity (κ_l) for $Cu_2CdSnSe_4$ nanocomposite materials.

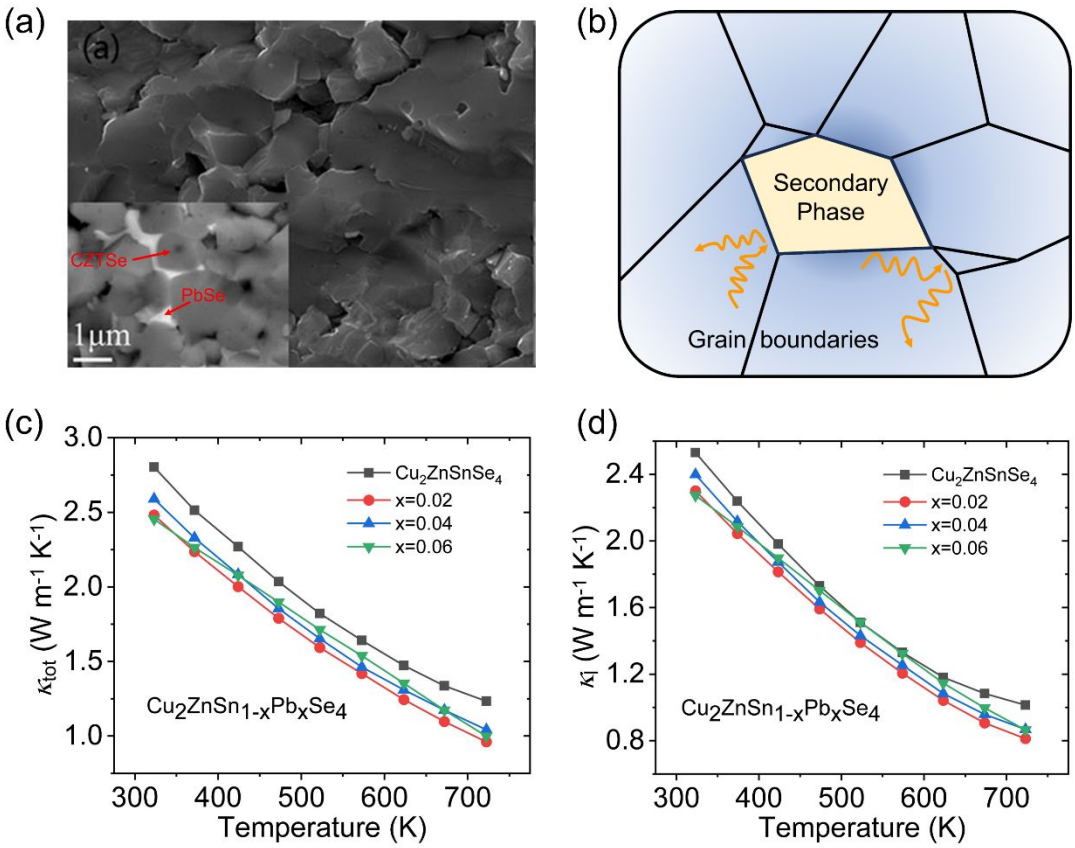

Figure 9 The structure and thermal properties of $Cu_2ZnSn_{1-x}Pb_xSe_4$. (a) SEM image of $Cu_2ZnSn_{1-x}Pb_xSe_4$. (b) Schematic diagram of secondary phase boundary scattering. Temperature dependence of (c) total thermal conductivity (κ_{tot}) and (d) lattice thermal conductivity (κ_l) of $Cu_2ZnSn_{1-x}Pb_xSe_4$.

Table1 Space group,band gap and *ZT* of Cu-based quaternary diamondoid compounds

Chemical formula	Space group	E_g (eV)	*ZT*, T(K)	Ref.
Cu_2ZnSnS_4	I-42m	1.4	0.36, 700	[42]
Cu_2ZnGeS_4	I-42m	2.05	/	[73]
$Cu_2ZnSnSe_4$	I-42m	1.41	0.95, 850	[42]
$Cu_2CdSnSe_4$	I-42m	0.96	0.65, 700	[34]
$Cu_2HgSnSe_4$	I-42m	1.81	0.2, 723	[74]
$Cu_2MgSnSe_4$	I-42m	1.7	0.42, 700	[75]
$Cu_2CdGeSe_4$	I-42m	1.2	0.42, 723	[76]
$Cu_2ZnGeSe_4$	I-42m	1.4	0.55, 723	[77]